(2)

PROGRESS REPORT

RESEARCH ON THE MICROSTRUCTURE OF RAPIDLY SOLIDIFIED ALLOYS

D. SHECHTMAN, L. A. BENDERSKY, AND E. HOROWITZ

THE JOHNS HOPKINS UNIVERSITY
CENTER FOR MATERIALS RESEARCH
G. W. C. WHITING SCHOOL OF ENGINEERING
BALTIMORE, MARYLAND 21218

APPROVED FOR PUBLIC RELEASE
DISTRIBUTION UNLIMITED

DARPA ORDER NO. MDA 903-83-K-0400
EFFECTIVE DATE: 08-05-83
EXPIRATION DATE: 08-04-85
SPONSORED BY: DEFENSE ADVANCED RESEARCH PROJECTS AGENCY (DARPA)

JUNE 1985

SECURITY CLASSIFICATION OF THIS PAGE (When Data Entered)

REPORT DOCUMENTATION PAGE

READ INSTRUCTIONS BEFORE COMPLETING FORM

1. REPORT NUMBER: CMR-DARPA-10	2. GOVT ACCESSION NO.: AD-A157 077
3. RECIPIENT'S CATALOG NUMBER:	
4. TITLE (and Subtitle): Research on the Microstructure of Rapidly Solidified Alloys	5. TYPE OF REPORT & PERIOD COVERED: Progress Report
	6. PERFORMING ORG. REPORT NUMBER:
7. AUTHOR(s): D. Shechtman, L. A. Bendersky, and E. Horowitz	8. CONTRACT OR GRANT NUMBER(s): MDA-903-83-K-0400
9. PERFORMING ORGANIZATION NAME AND ADDRESS: The Johns Hopkins University, Center for Materials Research, Baltimore, Maryland 21218	10. PROGRAM ELEMENT, PROJECT, TASK AREA & WORK UNIT NUMBERS:
11. CONTROLLING OFFICE NAME AND ADDRESS: DARPA, 1400 Wilson Blvd., Arlington, Va. 22209	12. REPORT DATE: June 1985
	13. NUMBER OF PAGES: 53
14. MONITORING AGENCY NAME & ADDRESS (if different from Controlling Office): ONRRR, George Washington University, 2110 G Street, SW, Washington, D. C. 20037	15. SECURITY CLASS. (of this report): A
	15a. DECLASSIFICATION/DOWNGRADING SCHEDULE:

16. DISTRIBUTION STATEMENT (of this Report)

Approved for public release, distribution unlimited

17. DISTRIBUTION STATEMENT (of the abstract entered in Block 20, if different from Report)

18. SUPPLEMENTARY NOTES

Keywords:

19. KEY WORDS (Continue on reverse side if necessary and identify by block number)

Microstructure, Icosahedral Quasicrystal, Related Phases, Variations in Melt Spun RS Microstructures, Metastable Phases in Al-Rich Fe Alloys, Microstructure of Selected RS Alloys: Al-Mn, Co-34wt%Sn, and Al-3.7wt%Ni-1.5wt%Fe.

20. ABSTRACT (Continue on reverse side if necessary and identify by block number)

The results of research performed on rapidly solidified alloys are presented. A major breakthrough by Shechtman is reported in the first paper on Al-Mn alloys with a metallic phase (icosahedral quasicrystal) with long range orientational order and no translational symmetry. Several other papers related to this newly discovered phase are also included. In addition, the microstructure and phases in other rapidly solidified alloys are discussed including variations in microstructure as a function of processing conditions.

DD FORM 1 JAN 73 1473 EDITION OF 1 NOV 65 IS OBSOLETE

TABLE OF CONTENTS

FIGURES

FIGURES

FIGURES

FIGURES

TABLES

EXECUTIVE SUMMARY

This progress report presents research performed for the Defense Advanced Research Projects Agency (DARPA) under contract no. MDA903-83-K-0400. The discovery of the icosahedral phase in aluminum-manganese alloys by Shechtman (I), while performing research on the microstructure of rapidly solidified alloys under a contract by the Defense Advanced Research Projects Agency (DARPA) to The Johns Hopkins University has created world wide interest in this new form of matter. This research was also performed under a cooperative research agreement between The Johns Hopkins University and the National Bureau of Standards Center for Materials Science which has made it possible for Johns Hopkins faculty and staff to conduct experiments at NBS as guest workers using their outstanding facilities. There has also been an extremely useful and productive interaction between NBS scientists and Johns Hopkins personnel which has enriched the experimental and theoretical aspects of the work.

Since the original discovery by Shechtman, there has been an even stronger effort and commitment by the Johns Hopkins and NBS groups to work closely on problems of mutual interest. This is a fine example of an outstanding government laboratory (NBS) working synergistically with a university to facilitate the accomplishment of mutual goals.

The "Metallic Phase with Long-Range Orientational Order and No Translational Symmetry" is the classic work (I)

by Shechtman, et al. on the newly discovered icosahedral phase which forms during rapid cooling from the melt. On the basis of experiments performed in the course of this study the presence of multiple twinned crystals was ruled out.

The manuscript on "Nuclear Gamma-Ray Resonance Observations in Aluminum-Based Icosahedral Quasicrystals" (II) provides additional experimental evidence for the icosahedral crystalline phase and supports a model based on quasi-periodic filling of space by rhombehedra with two different shapes filling space in a quasiperiodic way.

The similarity of structure between the icosahedral phase and the previously cited T phase and the Al_4Mn phase is investigated using transmission electron microscopy and discussed in the paper "Icosahedral Al-Mn and Related Phases: Resemblance in Structure" (III). Another phase, globular in form with 5-fold symmetry but different from the icosahedral phase, was observed and will be discussed in a subsequent paper. An interesting structural relationship appears to exist among the Al_4M, T and icosahedral phases.

The work on "Microstructural Variations in Melt-Spun Rapidly Solidified Ribbons" (IV) deals with the microstructural changes which occur in different alloys in different parts of the melt spun ribbon. The regions of the ribbons investigated were near the wheel side and in the center. Transmission electron microscopy was used in this study on the following specimens: Al-3.7Ni-1.5Fe(wt%), Co-34wt%Sn, and Nb-25at%Si.

Melt-spun ribbons of Co-34wt%Sn eutectic alloy were characterized by transmission electron microscopy and metallographically and compared to solid specimens obtained from bulk undercooling and later heat-treated. This study is reported in the "Microstructure of Rapidly Solidified Co-34at%Sn Eutectic Alloys" (V). The microstructure is described and includes columnar grains of supersaturated Co_3Sn martensite 2H phase (wheel side or whole ribbon) and supersaturated α-Co particles in DO_{19} (41wt%Sn) CO_3Sn hexagonal form. A discussion and explanation of the results is provided.

The paper by Shechtman and Swartzendruber, "Metastable Phases in Rapidly Solidified Aluminum-Rich Aℓ-Fe Alloys" (VI) is included in this progress report and describes the results for melt spun specimens including the structure of the metastable phase and microstructural transformations following controlled heat treatment.

Two papers are being prepared for the AMS/AIME meeting in October 1985 and abstracts of these publications are included in this report. The research to be reported includes:

1. "The Microstructure of Rapidly Solidified Aℓ-3.7wt%Ni-1.5wt%Fe" (VII).

   The specimens were subjected to electron beam passes at different speeds varying from 5 m/s to 1 mm/s. The influence of solidification velocity on the microstructure was studied and analyzed.

2. "Possible Structural Similarities between the Various Phases Produced in Aℓ-Mn Alloys Using a Range of Solidification Conditions" (VIII).

Two intermediate metastable phases of the alloy Aℓ-Mn are formed at slow cooling rates, and these are designated T and T'. Using transmission electron microscopy and other characterization techniques it was found that structural similarities exist among the icosahedral phase, $A\ell_4Mn$, T and T'. The microstructure of these phases will be described in some detail.

Metallic Phase with Long-Range Orientational Order and No Translational Symmetry

D. Shechtman and I. Blech
Department of Materials Engineering, Israel Institute of Technology—Technion, 3200 Haifa, Israel

and

D. Gratias
Centre d'Etudes de Chimie Métallurgique, Centre National de la Recherche Scientifique, F-94400 Vitry, France

and

J. W. Cahn
Center for Materials Science, National Bureau of Standards, Gaithersburg, Maryland 20760
(Received 9 October 1984)

We have observed a metallic solid (Al–14-at.%-Mn) with long-range orientational order, but with icosahedral point group symmetry, which is inconsistent with lattice translations. Its diffraction spots are as sharp as those of crystals but cannot be indexed to any Bravais lattice. The solid is metastable and forms from the melt by a first-order transition.

PACS numbers: 61.50.Em, 61.55.Hg, 64.70.Ew

We report herein the existence of a metallic solid which diffracts electrons like a single crystal but has point group symmetery $m\bar{3}\bar{5}$ (icosahedral) which is inconsistent with lattice translations. If the specimen is rotated through the angles of this point group (Fig. 1), selected-area electron diffraction patterns clearly display the six fivefold, ten threefold, and fifteen twofold axes characteristic[1] of icosahedral symmetry (Fig. 2). Grains up to 2 μm in size with this structure form in rapidly cooled alloys of Al with 10–14 at.% Mn, Fe, or Cr. We will refer to the phase as the icosahedral phase. Microdiffraction from many different volume elements of a grain and dark-field imaging from various diffraction spots confirm that entire grains have long-range orientational order. If the orientational order decays with distance, its correlation length is far greater than the grain size. We have thus a solid metallic phase with no translational order and with with long-range orientational order.

The remarkable sharpness of the diffraction spots (Fig. 2) indicates a high coherency in the spatial interference, comparable to the one usually encountered in crystals. The diffraction data are qualitatively well fitted by a model consisting of a random packing of nonoverlapping parallel icosahedra attached by edges.[2] The invariance of the local orientational symmetry from site to site and the finite number of possible translations between two adjacent icosahedra seem to be sufficient for insuring highly coherent interferences. Icosahedra are a common packing unit in intermetallic crystals with the smaller transition element at the center surrounded by twelve larger atoms arranged like the corners of an icosahedron.[3] The symmetries of the crystals dictate that the several icosahedra in a unit cell have different orientations and allow them to be distorted, leaving the overall crystal consistent with the well-known crystallographic point and space groups. Even though icosahedral symmetry is of great importance as an approximate site symmetry in crystals, it cannot survive the imposition of lattice translations: Crystals cannot and do not exhibit the icosahedral point group symmetry.

Elementary crystallography indicates that fivefold

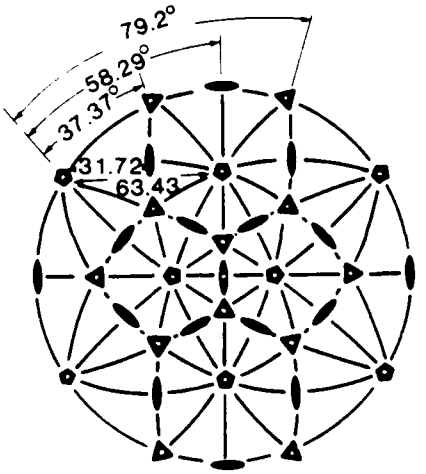

FIG. 1. Stereographic projection of the symmetry elements of the icosahedral group $m\bar{3}\bar{5}$.

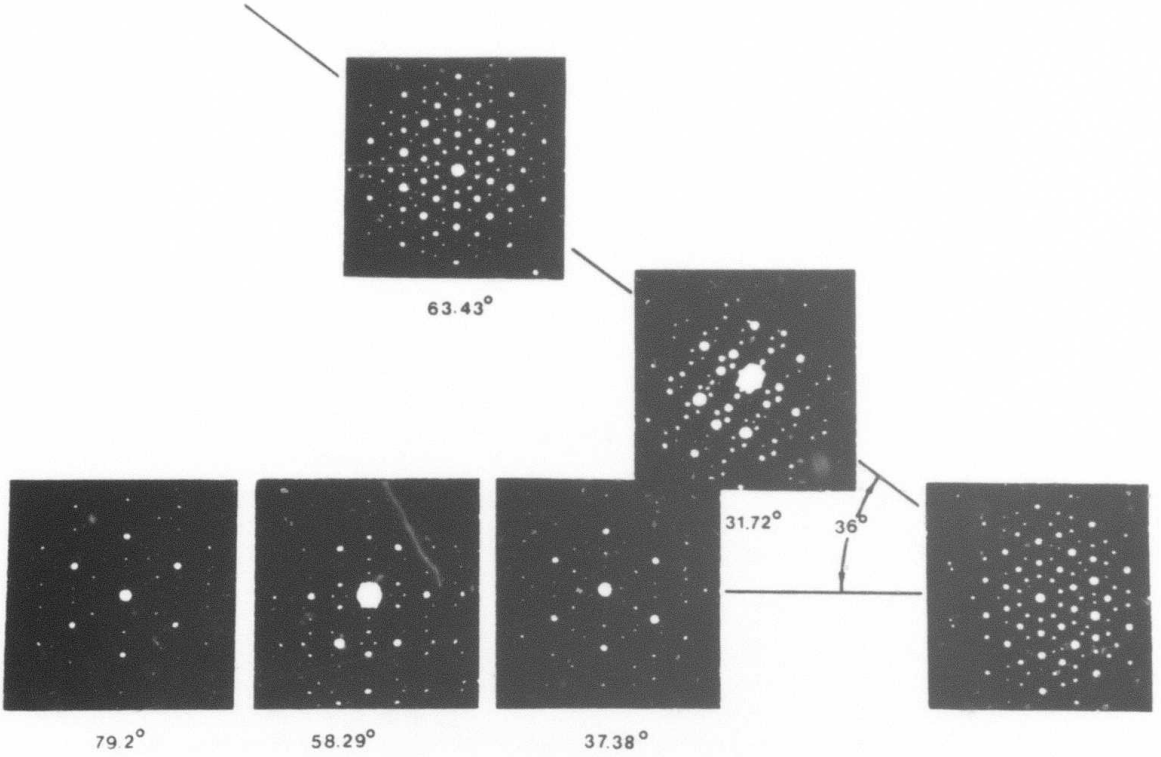

FIG. 2. Selected-area electron diffraction patterns taken from a single grain of the icosahedral phase. Rotations match those in Fig. 1.

axes are inconsistent with translational order.[4] Crystals with an apparent fivefold axis do occur as multiple twins.[5] Icosahedral symmetry could conceivably occur by multiple twinning, but at least five twins are required in order to obtain an icosahedral diffraction set from a conventional crystal. Experiments in the electron microscope and with x-ray diffraction contradict the twin hypothesis:

(1) A set of dark-field images taken from any reflection reveals no twins and in all cases the whole grain is illuminated.

(2) A convergent-beam diffraction pattern along the fivefold zone taken from an area 20 nm in diameter at any point of the grain displays all the reflections that appear in the selected-area diffraction pattern. This is also true when the thickness of the specimen is of the order of 10 nm.

(3) An x-ray diffraction pattern (Cu $K\alpha$ source) was taken from a single-phase sample of the material containing many grains of various orientations. Had the phase consisted of a multiply twinned crystalline structure, it should have been possible to index the powder pattern regardless of the twins. The pattern obtained from the icosahedral phase could not be indexed to any Bravais lattice.

On the basis of these experiments we conclude that the icosahedral phase does not consist of multiply twinned regular crystal structures.

The icosahedral phase forms during rapid cooling of the melt by a nucleation and growth mechanism. This mechanism is characteristic of a first-order transition because the two phases coexist along a moving interface. Each particle nucleates at a center and grows out from there. The atomic rearrangements that result in the orientational order of the icosahedral phase occur at this interface, and the two adjoining phases differ in entropy and, for some alloys, in composition. If the transition were higher order, ordering would occur everywhere in the liquid instead of being confined to interfaces. Our evidence for the first-order character is morphological. We examined alloys with 10–14 at.% Mn. Samples with 10% to 12% Mn showed many nodular grains separated from each other by crystalline films of fcc Al. The grains were approximately spherical in shape but were deeply indented with radial streaks composed of fcc Al crystals. The morphology is similar to a commonly observed one in rapid solidification in which crystals nucleate at

many centers and grow until the remaining liquid solidifies, except that instead of isolated crystals we have isolated icosahedral grains embedded in solidified Al.

Another aspect of the first-order character of the transition is that segregation accompanies the growth of the icosahedral phase. In the 10%- and 12%-Mn samples the growing phase rejects Al into the liquid. The indentations in the nodules are characteristic of the cellular morphology caused by an instability in the diffusion layer surrounding the solid resulting from segregation during growth.[6] In the 14%-Mn alloys the icosahedral grains occupy almost all of the volume of the specimen. Only small amounts of fcc Al occur along some grain boundaries where the grains grew to impingement. Some radial streaking still points to the nucleation centers from which the grains grew. We conclude that little segregation occurs in this alloy and that the icosahedral phase contains 14% Mn.

The obvious cellular morphology indicates that the growth of the icosahedral phase is slow enough to permit diffusional segregation on the scale of 1 μm. With the diffusion coefficient in the liqud of order 10^{-8} m^2/s this indicates interface velocities of order 10^{-2} m/s and formation times of 10^{-4} s. This is 2 to 3 orders of magnitude slower than the fastest known crystallization velocities of a metallic liquid during rapid cooling, but it is a typical upper limit of velocity of crystallization with composition changes.[7] There is thus plenty of time for atomic rearrangements to occur at the interface between the melt and the icosahedral phase.

The icosahedral phase in rapidly solidified Al-Mn alloys is remarkably resistant to crystallization. Prolonged heating of 6 h at 300 °C and 1 h at 350 °C produced no detectable crystallization, but 1 h at 400 °C caused crystallization to the stable Al_6Mn phase. We conclude that the icosahedral phase is a truly metastable phase which nucleates and grows for a range of cooling rates which are slow enough to permit its formation but rapid enough to prevent crystallization, either from the melt or from the icosahedral phase after its formation.

The icosahedral phase has symmetries intermediate between those of a crystal and a liquid. It differs from other intermediate phases in that it is both solid, like a metallic glass, and that it has long-range orientational order. Many intermediate phases do have orientational order, but usually it is only local, and the transition to such phases is continuous.[8,9] The possibility of an icosahedral phase with long range order was inferred from a computer simulation,[10,11] and a first-order liquid-to-icosahedral phase transition has been predicted from a mean-field theory.[11,12]

We thank F. S. Biancaniello for spinning the alloys, C. R. Hubbard for x-ray experiments, and B. Burton for a critical review of the manuscript. This work was sponsored by the Defense Advanced Research Projects Agency and the National Science Foundation. This work was performed while one of us (D.S.) was a guest worker at the National Bureau of Standards and while another of us (D.G.) was at the Institute for Theoretical Physics, University of California at Santa Barbara.

[1] *International Tables for Crystallography* (Reidel, Higham, Mass., 1983), Vol. A, p. 179.

[2] D. Shechtman and I. Blech, to be published.

[3] F. C. Frank and J. S. Kasper, Acta Crystallogr. **11**, 184 (1958), and **12**, 483 (1959).

[4] M. J. Buerger, *Elementary Crystallography* (MIT Press, Cambridge, 1978).

[5] G. Friedel, *Lecon de Crystallographie* (Masson, Paris, 1921).

[6] W. W. Mullins and R. F. Sekerka, J. Appl. Phys. **35**, 444 (1963).

[7] W. J. Boettinger, F. S. Biancaniello, G. Kalonji, and J. W. Cahn, in *Rapid Solidification Processing II*, edited by R. Mehrabian *et al.* (Claitors, Baton Rouge, 1980), p. 50.

[8] D. R. Nelson, Phys. Rev. B **28**, 5515 (1983).

[9] J. Sadoc, J. Phys. (Paris), Colloq. **41**, C8-326 (1980).

[10] P. J. Steinhardt, D. R. Nelson and M. Rouchetti, Phys. Rev. Lett. **47**, 1297 (1981).

[11] P. J. Steinhardt, D. R. Nelson and M. Rouchetti, Phys. Rev. B **28**, 784 (1983).

[12] A. D. J. Haymet, Phys. Rev. B **27**, 1725 (1983).

NUCLEAR GAMMA-RAY RESONANCE OBSERVATIONS IN AN ALUMINUM-BASED ICOSAHEDRAL QUASICRYSTAL

L. J. Swartzendruber,# D. Shechtman,*+ L. Bendersky,+ and J. W. Cahn#

Center for Materials Science
National Bureau of Standards
Gaithersburg, Md.

* Department of Materials Engineering
Israel Institute of Technology
Technion, 32000 Haifa Israel

+ Center for Materials Research
The Johns Hopkins University
Baltimore, Md.

To be published in Physics Review B.

Nuclear gamma-ray resonance (Mössbauer effect) results are presented from rapidly solidified Aℓ-(Mn,Fe) alloys which contain the orientationally ordered phase with icosahedral point group symmetry. Detailed analysis of the spectra obtained are consistent with an icosahedral quasi-crystalline model for the structure of this phase.

It has recently been shown[1] that rapid solidification of Aℓ-rich Aℓ-Mn alloys by melt spinning can produce a metallic solid which diffracts electrons like a single crystal but has point group symmetry $m\bar{3}\bar{5}$ (icosahedral) which is inconsistent with lattice translations. Following Ref. 1 we refer to this phase as the icosahedral phase. It has long range orientational order giving rise to sharp diffraction patterns, but lacks periodic translational order. It is a metastable phase which forms by a first order transition. Once formed, heating above 350°C is required for it to crystallize to the stable $Aℓ_6Mn$ phase.

Thus far two models have been proposed which claim to explain the observed diffraction patterns from this icosahedral phase. One model consists of a packing of parallel icosahedra attached by the edges, each containing one transition metal atom at its center.[2] The second proposes a quasi-periodic filling of space by rhombohedra with two distinct shapes filling space in a quasiperiodic manner.[3,4] We present here nuclear gamma-ray resonance (NGR) data that are incompatible with the first model and which, at the same time, are consistent with the present form of the second model.

The icosahedral phase has been found to form readily in melt-spun Aℓ-rich Aℓ-Mn alloys,[1] but only in small amounts in melt-spun Aℓ-rich Aℓ-Fe alloys. In order to observe the NGR of ^{57}Fe, ternary alloys were used. Two melt-spun ribbons were prepared with the compositions (in weight %) Aℓ-22 Mn-4 Fe

and Aℓ-16 Mn-10 Fe. These correspond to the formulas $Aℓ_6(Mn_{0.85}Fe_{0.15})_{1.03}$ and $Aℓ_6(Mn_{0.62}Fe_{0.38})_{1.03}$, respectively. These two alloys produced essentially identical spectra. Optical microscopy on cross section and transmission electron microscope (TEM) examination on thin foils of this alloy showed only two phases: the icosahedral phase and a small amount of fcc Aℓ. Electron and x-ray diffraction patterns from this icosahedral phase were indistinguishable from those published[6] for the binary Aℓ-Mn alloy. Since Fe is known to be insoluble in fcc Aℓ (less than 3 at% dissolves at the highest achievable quenching rates[7], and considering the small amount of fcc Aℓ present, we believe it is valid to assume that nearly all of the Fe atoms in the as-spun ternary alloys reside as random substitutions for Mn atoms in the icosahedral phase. Contributions to the observed NGR spectra from other phases will be insignificant.

The as-spun alloys were also heat treated in vacuum at 500°C for 1 hour. TEM examination after this heat treatment revealed that all the icosahedral phase has transformed to the crystalline $Aℓ_6Mn$ structure.

The model based on iron atoms centered in aluminum icosahedra is inconsistent with the rather strong quadrupole splitting in the observed spectra (see Fig. 1). Icosahedral first-neighbor coordination of the transition metal atoms would imply high local symmetry[8] resulting in little or no electric field

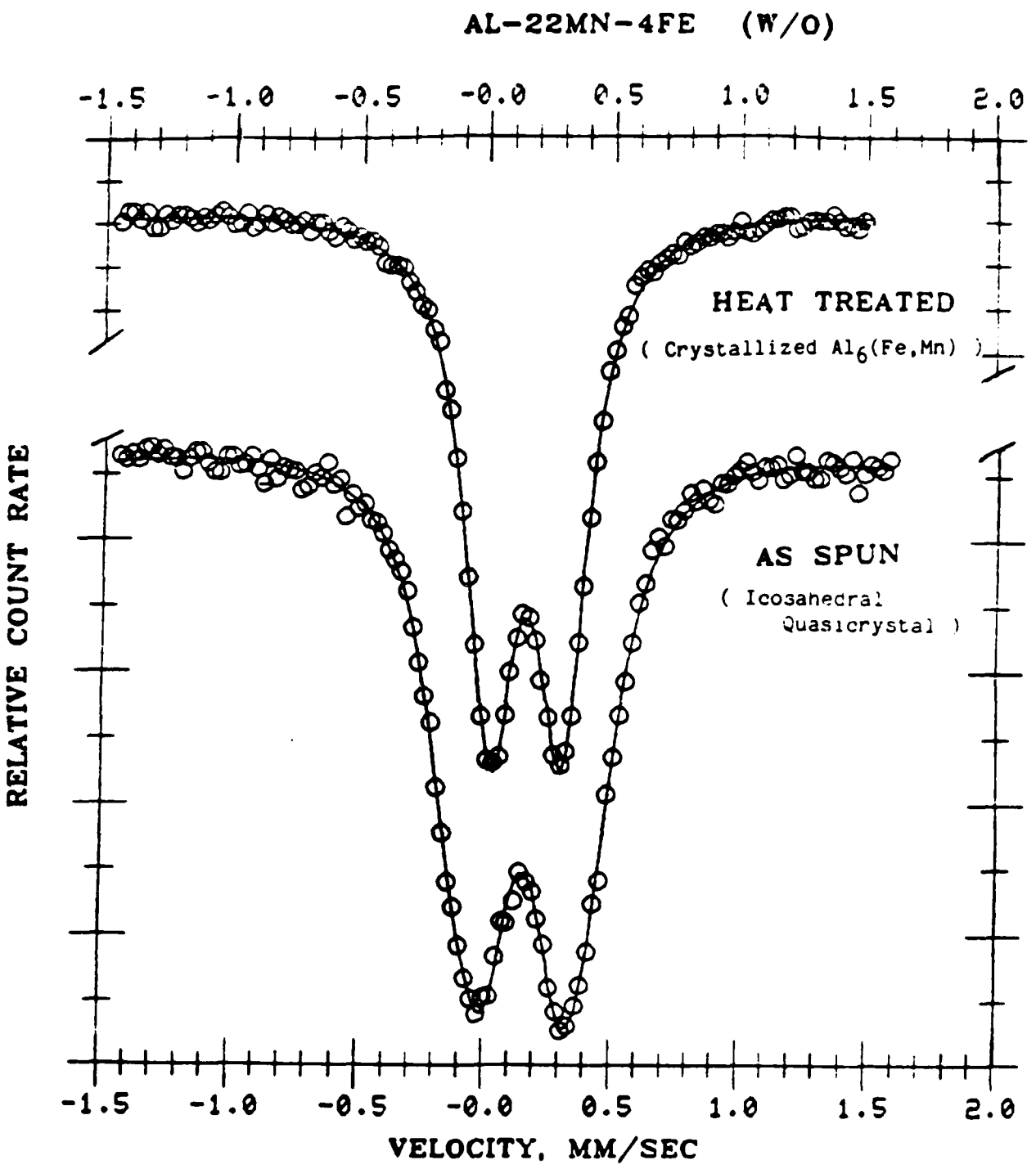

Figure 1. Room temperature NGR absorption spectra from the heat treated (crystallized) and from the as-spun (quasicrystal) alloy $Al_6(Mn_{0.85}Fe_{0.15})_{10.3}$. The circles are data points and the solid line is the least squares fit obtained as described in the text. The zero of velocity represents the center of a pure iron spectrum at room temperature and positive velocity represents source and absorber approaching.

gradient from asymmetries in the second- and further-neighbor coordination shells would be insufficient to produce the observed splitting.

In the quasi-crystalline model proposed by Levine and Steinhardt[3] a quasi-periodic structure is generated using a pair of polyhedra which are the three-dimensional analogues of the two-dimensional Penrose tiles.[4,9,10] These two polyhedra form a space-filling quasilattice of infinite extent which is nonperiodic and from which a diffraction pattern can be calculated.[3,11] The calculated pattern[3] is consistent with the 3- and 5-fold symmetry, spacing, intensity, and sharpness in the observed pattern[1,2] (although the positions of the atoms in this structure have not been determined). In filling all space, the two polyhedra must occur in the ratio 1.618.. to 1 (the golden mean) with the more frequent polyhedron being less distorted than the less frequent one. In Mackay's rhombic triacontahedron the two polyhedra occur in equal numbers.[9] Packing these two kinds of polyhedra leads to a quasi-crystalline lattice which is self similar in the sense that one can eliminate a subset of lattice points and increase all distance scales by a constant factor to obtain another quasi-crystalline lattice. This inflation procedure can be reversed but it must cease to have validity beyond the point where the number of transition metal atoms per quasi-lattice point or polyhedron becomes 1. We therefore assume that there are two kinds of asymmetric sites for the transition metal atoms and that the ratio for

the numbers of atoms of each kind should be the golden mean. This would produce an NGR spectrum consisting of two quadrupole doublets with a golden mean amplitude ratio.

The spectra obtained for the $Al_6(Mn_{0.85}Fe_{0.15})_{1.03}$ alloy both as spun and after heat treatment are shown in Fig. 1. The spectrum from the heat treated sample has been least squares fitted to a symmetric doublet. The parameters obtained are given in Table 1. The value obtained for the quadrupole splitting, 0.287 mm/sec, can be considered identical to the 0.288 mm/sec splitting observed previously by Stickels and Bush[6] in metastable Al_6Fe. The linewidth, 0.244 mm/sec, is only slightly greater than the natural line-width for ^{57}Fe (0.21 mm/sec) and the slight broadening is largely attributable to instrumental effects ($\approx$ 0.02 mm/sec). By fitting to separate lines it was determined that this doublet is, within experimental error, completely symmetric.

The spectrum obtained for the as-spun icosahedral sample (Fig. 1) was least-squares fitted to a pair of symmetric doublets. In the least-squares fit the height ratio of the two doublets was constrained to be 1.618. All other parameters, i.e., the isomer shifts, linewidth, and quadrupole splittings, were unconstrained. The parameters obtained from this fit are shown in Table 1. Note that the more intense doublet, which we associate with the less distorted polyhedron, has an isomer shift and quadrupole splitting very close to that observed for

Table 1

Parameters obtained by least-squares fitting the spectra of Fig. 1 for $Al_6(Mn_{0.85}Fe_{0.95})_{1.03}$ and for a sample of $Al_6(Mn_{0.62}Fe_{0.38})_{1.03}$. Isomer shifts are given with respect to pure iron at room temperature.

Sample	Doublet 1				Doublet 2			
	Relative Intensity	Splitting mm/sec	Isomer Shift mm/sec	Width mm/sec	Relative Intensity	Splitting mm/sec	Isomer Shift mm/sec	Width mm/sec
Crystallized ($Fe_{0.15}$)	1.0	0.287	0.152	0.244	0	-	-	-
As spun ($Fe_{0.38}$)	1.618	0.298	0.150	0.289	1	0.550	0.141	0.272
Crystallized ($Fe_{0.38}$)	1.0	0.296	0.185	0.239	0	-	-	-
As spun ($Fe_{0.38}$)	1.618	0.294	0.191	0.297	1	0.523	0.174	0.288

the Al_6Mn structure, whereas the less intense doublet, which we associate with the more distorted polyhedron, has a considerably larger quadrupole splitting. This larger splitting indicates a larger electric field gradient. It can be noted that this type of two doublet fit gave a significantly lower residual standard deviation (0.14% compared to 0.22% at a count level of 6.3×10^5) than did an unconstrained fit to two individual lines. Attempts at fitting were also made using other doublet intensity ratios. For ratios of 1.8 and 1.4 the residual standard deviations were slightly larger although the difference could not be considered significant. At ratios of 2.0 and 1.2 the deviations were significantly larger. An equally valid fit was obtained when the linewidths of the two doublets were constrained to be equal. In that case the linewidth obtained was 0.286 mm/sec which is between linewidths given in Table 1. The larger linewidth in the quasicrystal over that in the crystallized material has two likely causes: (1) variations in the second and third near-neighbor environments expected in a nonperiodic quasicrystal, and (2) the presence of vacancies and other defects expected in a rapidly quenched crystal.

The NGR spectrum of an iron atom is essentially a probe of the local environment of that atom, being most sensitive to the first one or two near neighbor shells. Although the spectra obtained here do not establish the location of the Fe atoms in the crystal, they are consistent with the quasicrystalline model

of Levine and Steinhardt[3] and are not consistent with the model in which the Fe atoms are at centers of icosahedra.

ACKNOWLEDGEMENTS

We thank F. S. Biancaniello for preparing the alloy specimens, R. J. Schaefer for confirming which phases were present by x-ray diffraction, and P. J. Steinhardt for providing us with the geometry of the space-filling polyhedra used in the quasi-crystalline model. This work was partially supported by the Defense Advanced Research Projects Agency and was performed while two of us (D. S. and L. B.) were on a joint NBS-Johns Hopkins cooperative research program.

REFERENCES

1. D. Shechtman, I. Blech, D. Gratias, and J. W. Cahn, Phys. Rev. Lett. 53, 1951 (1984).

2. D. Shechtman and I. Blech, submitted to Met. Trans.

3. D. Levine and P. J. Steinhardt, Phys. Rev. Lett. (1984).

4. P. Kramer and R. Neri, Acta Cryst. A40, 580 (1984).

5. D. Shechtman and L. J. Swartzendruber, to be published.

6. C. A. Stickels and R. M. Bush, Met. Trans. 2, 2031 (1984).

7. S. Nasu, U. Conser, P. H. Singu, and Y. Murkami, J. Phys. F 4, 124 (1974).

8. International Tables for Crystallography Volume A, p. 779, Reidel 1983.

9. R. Penrose, Bull, Ins. Maths. and Its Appl. 10, No. 7/8, 266 (1974): see also M. Gardner, Sci. Am. 236, 110 (1977).

10. A. L. Mackay, Physica 114A, 609 (1982).

11. A. Katz and M. Duneau, Proceedings of Workshop on Mathematical Crystallography, I. H. E. S. Buressur Yvette, France, February 1985.

ICOSAHEDRAL Al-Mn AND RELATED PHASES: RESEMBLANCE IN STRUCTURE

L. Bendersky*, R. J. Schaefer, F. S. Biancaniello,
W. J. Boettinger, M. J. Kaufman, and D. Shechtman**
Metallurgy Division, National Bureau of Standards,
Gaithersburg, Md. 20899

INTRODUCTION

An icosahedral phase showing non-crystallographic point group symmetry $m\bar{3}\bar{5}$ and at the same time sharp single crystal-like electron diffraction has recently been reported [1]. In Al-Mn alloys, the phase is formed at alloy compositions between 15 and 35 wt% Mn. Several different techniques of rapid solidification provide sufficient melt undercooling to produce this phase. The icosahedral phase has been found to solidify in conjunction with other phases [2]. One of these phases, called T phase, was previously reported as a product of solid state precipitation [3] and is of interest due to the striking resemblance of electron diffraction patterns obtained from this phase and the icosahedral phase. The T phase is highly faulted, and the intermetallic Al_4Mn phase is found to be the unfaulted variant. Al_4Mn is a stable hexagonal phase with a large unit cell (a = 2.84 nm, c = 1.24 nm) [4,5], however, no additional structural information

*L. Bendersky is also with the Center for Materials Research, The Johns Hopkins University, Baltimore, Md. 21218.

**D. Shechtman is with the Department of Materials Engineering, Technion, Haifa, Israel, and the Center for Materials Research, The Johns Hopkins University, Baltimore, Md. 21218.

To be published in Scripta Metallurgica.

is available. In the present paper we report preliminary studies of the crystallographic relationship between these phases: icosahedral, T and Al_4Mn. The study was performed using conventional and high-resolution transmission electron microscopy.

ICOSAHEDRAL AND T PHASE

The coexistence of the icosahedral and the T phase was observed in two morphological forms. The first morphology is a mixture of the phases which exist for Al-25 wt% Mn in electron beam surface melts scanned at velocities between 50 and 200 cm/s. The icosahedral phase has the characteristic coral-like dendritic shape with mottled internal contrast (Figure 1), whereas the T phase appears as faceted blocky crystals with striated internal contrast associated with planar defects. In fact, in these samples a third phase was also observed, which has globular form and 5-fold diffraction symmetry, different from the icosahedral phase (Figure 2a, b). This phase, which we designate as T', is the subject of future investigation and will not be discussed further here. The second morphology is formed by the growth of T phase on the surface of icosahedral phase dendrites (Figure 3). Both morphologies suggest that the T phase replaces the icosahedral when the solidification velocity decreases. A strong orientation relationship between the two phases was observed for both morphologies.

The high-resolution image in Figure 4 is taken from a region in Figure 3 with the T phase adjacent to the icosahedral phase which was oriented along one of the two-fold axes. The interface

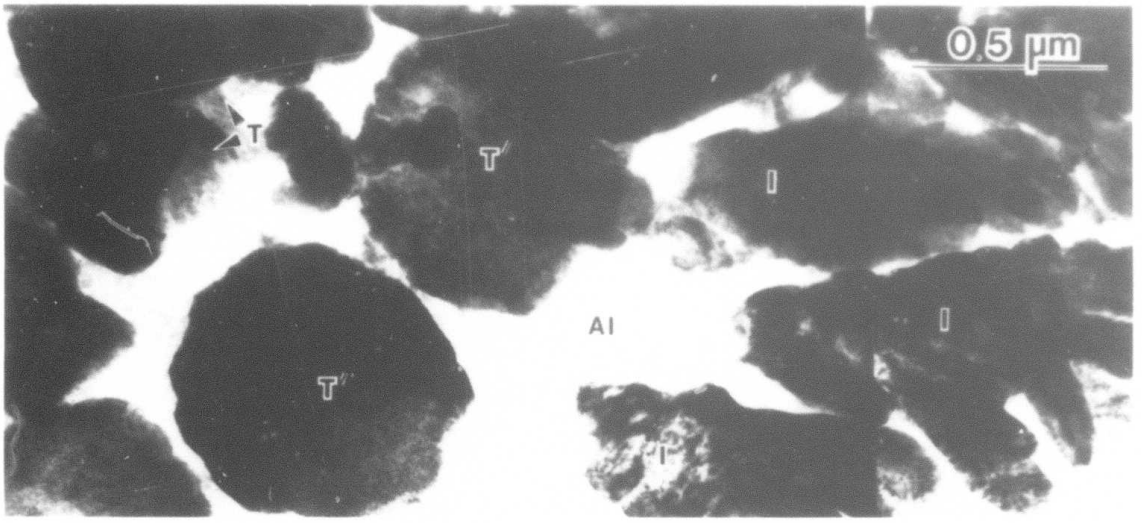

Figure 1. Microstructure of Aℓ-25 wt% Mn, electron beam surface melt scanned at velocity 200 cm/s. Arrows point on icosahedral (I), T, and T' phases.

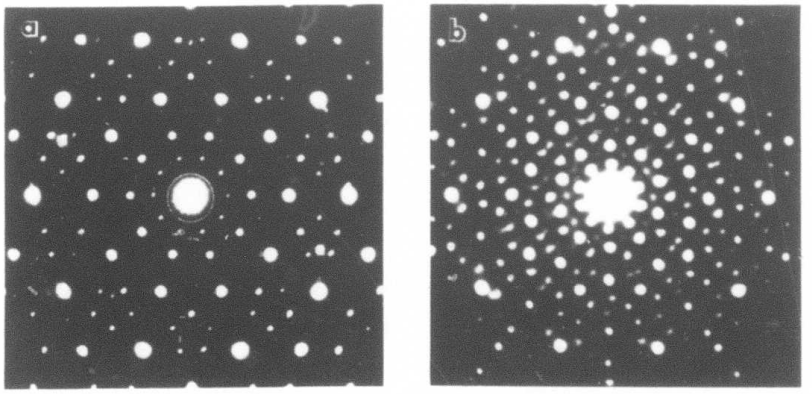

Figure 2. Diffraction patterns of icosahedral (a) and T' (b) phases at 5-fold symmetry zone axis orientation.

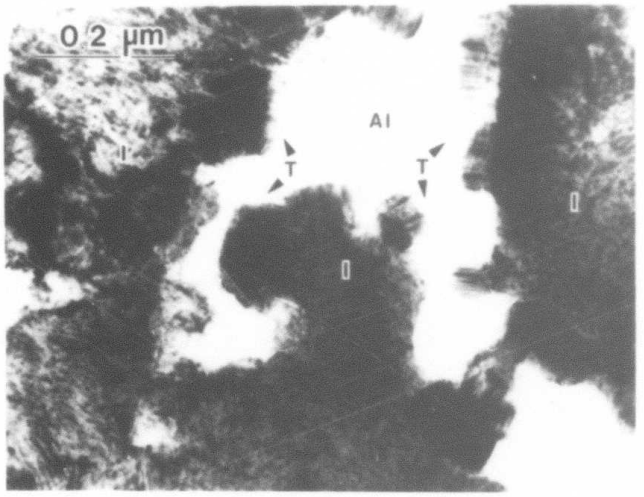

Figure 3. Growth of T phase on the icosahedral phase dendrites. Aℓ-27 wt% Mn melt spun ribbon.

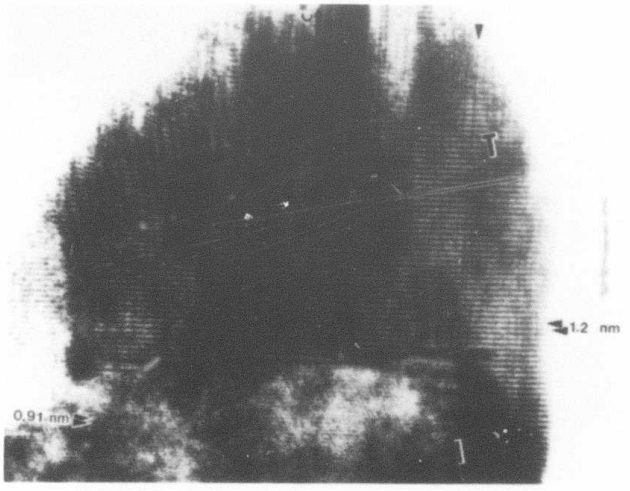

Figure 4. High-resolution image taken from the area shown on Figure 3. Epitaxial growth of T phase on icosahedral phase surface.

between these phases is sharp, suggesting that the phases differ by a first order transition. The T phase develops a periodic modulation (~1.2 nm) in the growth direction. No periodic modulations exist for the icosahedral phase. The observed periodic fringes are due to the limited number of beams used to form the high-resolution image. The structure of the T phase normal to the growth direction the structure is faulted and the diffraction shows streaking in the corresponding direction.

Figure 5 compares diffraction patterns for the icosahedral and T phases, where the pairs are chosen according to their orientation relationship. The "true" 5-fold symmetry diffraction pattern from the icosahedral phase (36° between radial rows of reflections) is comparable with the "almost" 5-fold diffraction pattern from the T phase, if one considers only the strongest reflections. For the T phase the angles between the ten radial directions are approximately 35° and 37°, and the spots are not exactly colinear. Nevertheless, the extinction and intensity distribution of spots for this phase are remarkably close to what is observed for the icosahedral phase. The same "matching" can be found for both 3-fold zone axes (Figure 5b) and several two-fold axes.

Due to the similarities of both the solidification conditions required to produce these phases and the electron diffraction patterns obtained from these phases, it is expected that a very close resemblance between the crystallographic structures exist. If the position of the atoms for T phase were known, then a set of

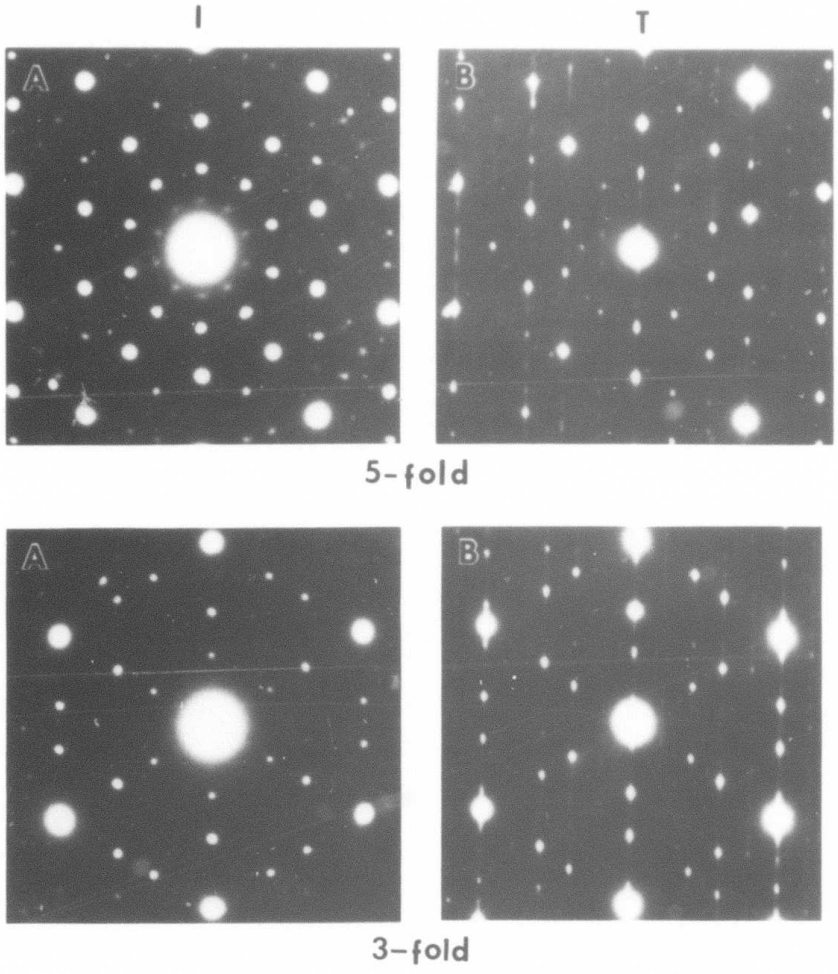

Figure 5. 5-fold and 3-fold symmetry diffraction patterns for icosahedral (a) and T (b) phases.

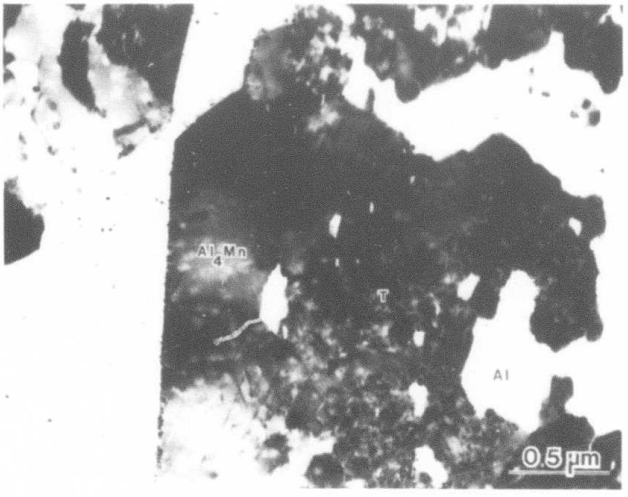

Figure 6. Microstructure of Aℓ-25 wt% Mn, electron beam surface melt scanned at velocity 1 cm/s. Low and high density defects areas are $A\ell_4Mn$ and T phase, respectively.

displacements could perhaps be found to satisfy all incommensurate modulations of the icosahedral phase; these modulations would necessarily eliminate the periodicity of the T phase. By this operation the planar defects would be destroyed and, accordingly, the streaking intensities eliminated.

T PHASE AND $A\ell_4Mn$

An analysis of the diffraction patterns obtained from annealed $A\ell_4Mn$ phase indicates that this phase is also similar to the T phase. In order to find a microstructural transition between these two phases, specimens were prepared by relatively slow velocity electron beam scans. Indeed, for Aℓ-25 wt% Mn melted with a scan velocity 1 cm/s, hexagon-like shaped crystals were found, showing a variable density of defects. Figure 6 shows one such crystal where areas can be seen which are almost defect-free and other areas containing a high density of defects. Diffraction patterns show the unfaulted area to be $A\ell_4Mn$. Diffraction patterns from faulted area are similar to those observed from the T phase. The faults were found to be (1100) planar defects.

A HREM image of the unfaulted part of $A\ell_4Mn$ is shown in Figure 7. This image was taken with the incident beam parallel to [0001] and at the objective lens set near the Scherzer focus. For a certain range of foil thicknesses the hexagonal arrangement of black dots, corresponding to the $A\ell_4Mn$ hexagonal lattice, is the most apparent feature of the image. The structure appears to be perfect, except for the planar defects A - A, B - B, and

C - C. These defects are of the same type mentioned above. Introducing this type of defect changes the basic structure very little, and probably the defects are antiphase boundaries with displacement vectors which effectively destroy the overall Al_4Mn superlattice. Indeed, Figure 8 shows the high resolution image of a faulted region, near an Al_4Mn region, which was identified by electron diffraction as T phase. The image was taken using conditions identical to those used in Figure 7, and hence the same type of black dots are imaged. Clear disorder of this structure is now present, except for small islands of Al_4Mn with a size of few unit cell dimensions.

Figure 9 compares diffraction patterns of Al_4Mn and T phase at the [0001] zone axis, used to obtain the high resolution images. The following can be concluded.

1. The disorder, introduced by the planar defects, results in an almost complete disappearance of the superlattice reflections of Al_4Mn and the appearance of diffuse intensity instead.

2. The character of the strong reflections along the A_i^* axis is maintained for the T phase, however the modulation changes from commensurate to incommensurate. The ratio of the g vector lengths along A_i^* for T phase is very close to the Golden ratio $\tau = (1 + \sqrt{5})/2$. τ is a characteristic number for icosahedral symmetry [6,7].

3. The T phase apparently has slightly different parameters lattice constants than Al_4Mn; this fact has been confirmed by x-ray diffraction [2]. This difference is probably due to the accommodation process of atoms at nonconservative APB's.

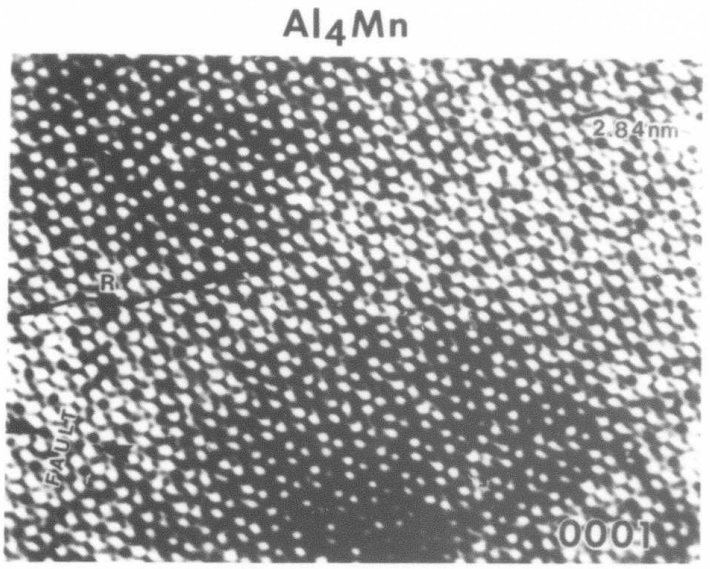

Figure 7. Structure image of Al_4Mn, viewed along [0001]. Antiphase boundary is observed.

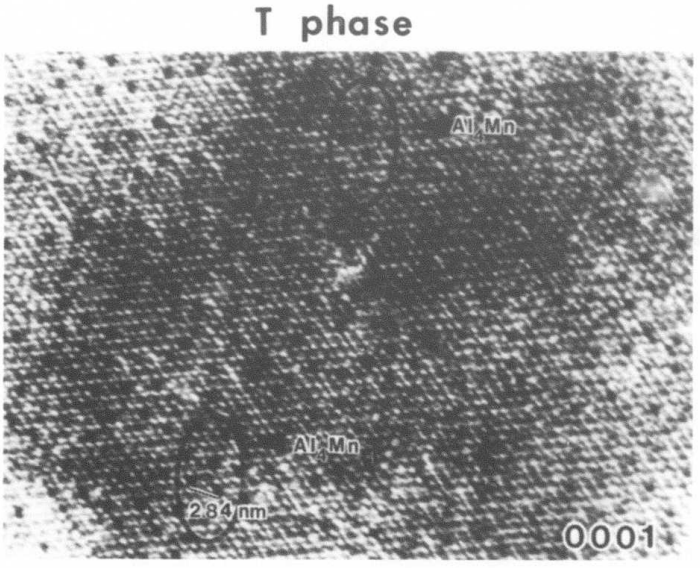

Figure 8. Structure image of T phase viewed along [0001].

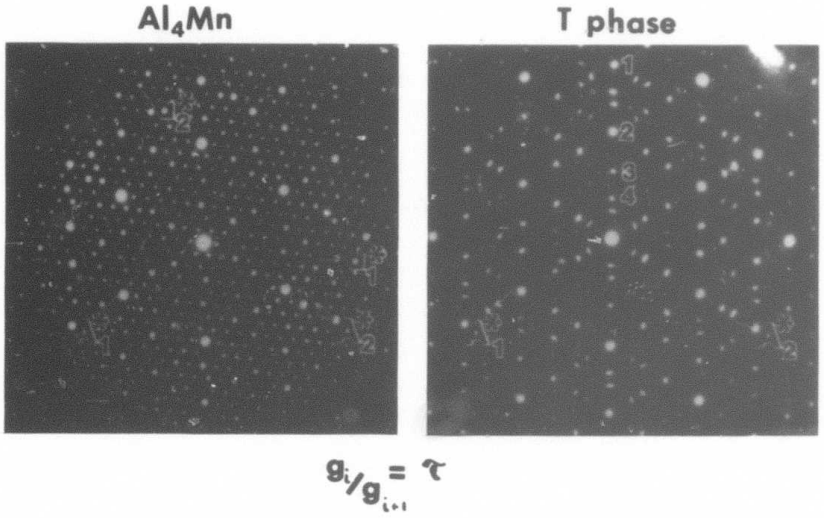

Figure 9. Diffraction patterns of $A\ell_4Mn$ (a) and T phase (b) at [0001] zone axis.

4. The T phase can be described as a two-dimensionally modulated structure ($A^*_{i,2}$ are the modulation directions) with a high density of irregular planar defects.

CONCLUSION

An analysis of electron diffraction patterns and high resolution images obtained from the three coexisting phases, Al_4Mn, T and icosahedral, indicates that a definite structural interrelationship exists between them. It is suggested that specific atomic displacements exist which transform one structure to another. This method may yield a natural way to approach the analysis of the noncrystallographic structure of the icosahedral phase. Unfortunately, the crystal structure of Al_4Mn is almost completely unknown and complicates this procedure. However, it may be established by standard procedures of x-ray structural analysis (this approach is currently being pursued).

ACKNOWLEDGEMENT

The authors thank DARPA for financial support of this work. Gratitude is expressed to J. W. Cahn and M. Kuriyama for helpful discussions and encouragement; and to C. H. Brady and D. Carrick for the specimen preparation.

REFERENCES

1. D. Shechtman, I. Blech, D. Gratias, J. W. Cahn, Phys. Rev. Let., 53, No. 20, 1951 (1984).
2. R. J. Schaefer, L. Bendersky, F. S. Biancaniello, W. J. Boettinger, D. Shechtman, to be published.
3. D. Shechtman, R. J. Schaefer, F. S. Biancaniello, Met. Trans A, 15A, 1987 (1984).
4. W. Hofmann, Aluminum, Berlin, 20, 865 (1938).
5. J. A. Bland, Thesis, University of Cambridge (1956).
6. International Tables for Crystallography (Reidel, Higham, MA (1983).
7. D. Levine, P. J. Steinhardt, Phys. Rev. Lett. 53, 2477 (1984).

MICROSTRUCTURAL VARIATIONS IN MELT-SPUN RAPIDLY SOLIDIFIED RIBBONS

L. A. BENDERSKY*+ AND W. J. BOETTINGER**

*Center for Materials Research, The Johns Hopkins University, Baltimore, Md. 21218

**Metallurgy Division, National Bureau of Standards, Gaithersburg, Md. 20899

Rapid solidification produces a wide variety of submicron scale microstructures. Generally, the microstructure depends on the imposed melt undercooling and heat extraction rate. The microstructure can vary strongly not only due to processing parameters changes but also during the process itself, as a result of recalescence. Hence, careful examination of different locations in rapidly solidified products should be performed. Additionally, post solidification solid-state reactions can alter the microstructure.

The objective of the present work is to demonstrate the strong microstructural changes in different regions of melt-spun ribbon for three different alloys. The locations of the analyzed structures were near the wheel side (W) and near the center (C) of the ribbons. The TEM specimens were prepared by selective electropolishing or ion milling.

Al-3.7 Ni-1.5 Fe (wt%) - The microstructure (W) shows columnar grains of α-Al with a uniform distribution of $Al_9(Fe,Ni)_2$ disc-like precipitates (Fig. 1a). A many variant orientation relationship has been established for this microstructure ($(001)_{Al} \| (031)p$) [1]. The microstructure is formed in two stages:

+Guest Worker, Metallurgy Division, National Bureau of Standards, Gaithersburg, Md. 20899

To be published in the Electron Microscopy Society of America.

(1) partitionless solidification of supersaturated α-Al; (2) precipitation of $Al_9(Fe,Ni)_2$ during subsequent cooling. The region C shows a cellular structure of α-Al with intercellular $Al_9(Fe,Ni)_2$ (Fig. 1b). A single variant orientation relationship has been found for this microstructure. This suggests that both phases were formed from the melt rather than by solid-state decomposition.

Co-34 wt% Sn - The microstructure W shows columnar grains of the nominal alloy composition, which are martensitically transformed (Fig. 2a). The martensite is a faulted 2H orthorhombic structure, and the plates are in a twin relation. The suggested mechanism of formation of the microstructure is: (1) partitionless solidification of high-temperature $Co_3Sn(DO_3)$ (not observed directly); (2) martensitic transformation $DO_3 \rightarrow 2H$ during subsequent cooling [2]. The microstructure C shows a very fine interconnected structure of α-Co(FCC) and an intermetallic phase, which has been identified as low temperature $Co_3Sn(DO_{19})$ (Fig. 2b). The microstructure may result from a reduction of the solidification velocity of the structure W due to recalescence. The conditions for the formation of interconnected structures in general require further investigation.

Nb-25 at% Si - The microstructure W shows a glassy phase. Away from the wheel side of the ribbon a mixture of glass with microcrystallites were observed (Fig. 3a). Glass formation is expected due to the deep eutectic (~ 20 at% Si) in Nb-Si phase diagram. The microstructure C shows a duplex structure

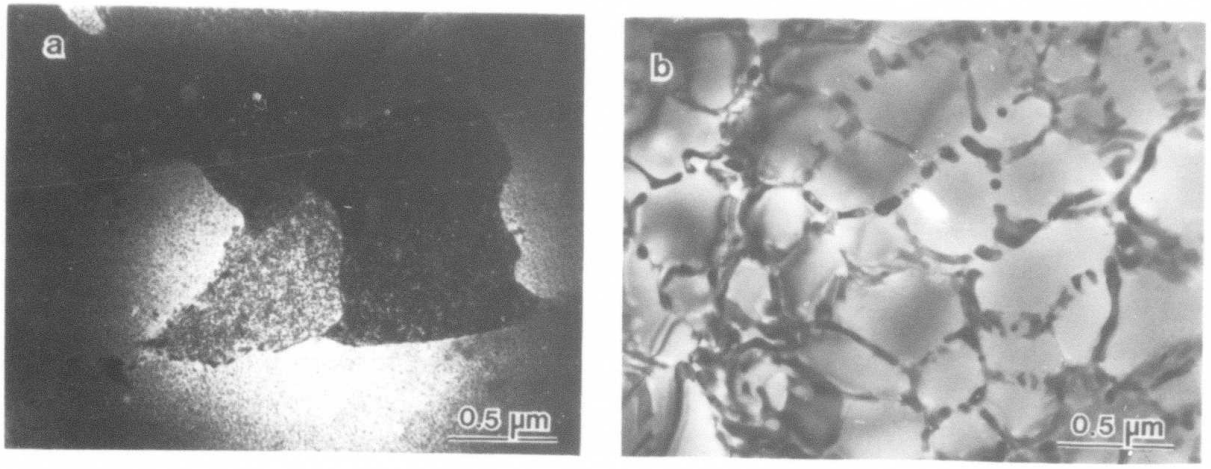

Fig. 1. Aℓ-3.7 Ni-1.5 Fe alloy. (a) $Aℓ_9(Fe,Ni)_2$ precipitates near the wheel side; (b) cellular α-Aℓ with $Aℓ_9(Fe,Ni)_2$ intercellular phase at the ribbon center.

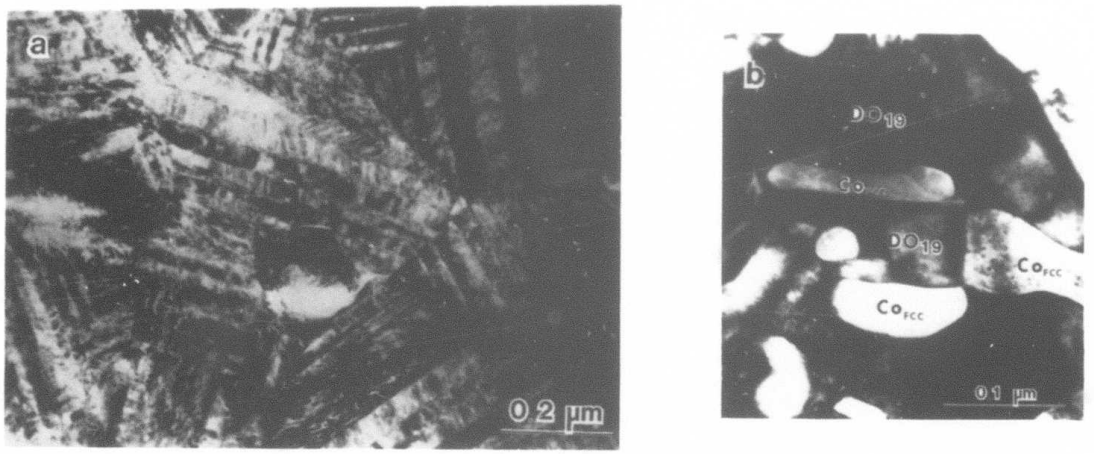

Fig. 2. Co-34 Sn alloy. (a) Martensitically transformed grains near the wheel side; (b) interlocked structure of α-Co and Co_3Sn at the ribbon center.

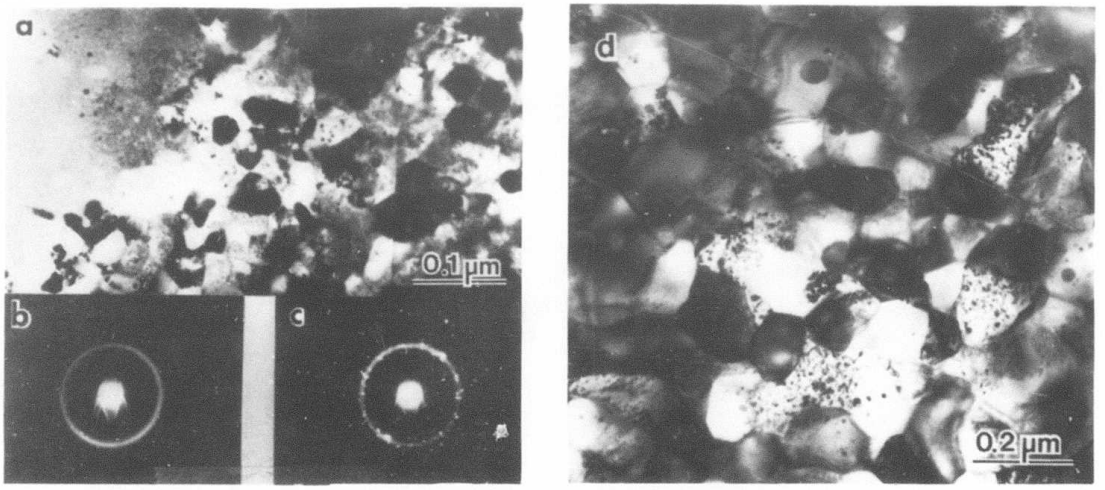

Fig. 3. Nb-25 at% Si. (a) Transition from glass to microcrystalline structure, near the wheel side; (b) (c) diffraction patterns showing transition; (d) microcrystalline structure of α-Nb and Nb_5Si_3 at the ribbon center.

of very fine, randomly oriented and equiaxed grains of α-Nb and Nb_5Si_3. The Nb_5Si_3 grains grow first, which can be concluded from interface curvatures. This structure requires a very high nucleation rate, assisted by a slow growth rate of the intermetallic phase. Subsequent nucleation (on numerous Nb_5Si_3 grains) and growth of α-Nb completes solidification.

REFERENCES

1. L. Bendersky, Met. Trans A, April 1985.

2. L. Bendersky, T. Z. Kattamis, F. S. Biancaniello, MRS Fall Meeting, Boston, p. 82, 1984.

This work was sponsored by the Defense Advanced Research Projects Agency (DARPA).

MICROSTRUCTURE OF RAPIDLY SOLIDIFIED Co-34wt%Sn EUTECTIC ALLOY

L. Bendersky, T. Z. Kattamis, and F. Biancaniello*

ABSTRACT

The microstructure of melt-spun ribbon of Co-34wt%Sn eutectic alloy was studied metallographically and by TEM and compared with that of specimens solidified from bulk-undercooled melts and subsequently heat-treated. The ribbon consists of columnar grains of a supersaturated Co_3Sn martensitic 2H phase. They occupy the whole thickness of the ribbon or the chill-side part of it, while the top part consists of a dispersion of supersaturated α-Co particles in a DO_{19} (41wt%Sn) Co_3Sn hexagonal structure. This dispersion is similar to that observed in bulk-undercooled alloys. An explanation is proposed based on the formation of a high temperature cubic DO_3 Co_3Sn during recalescence which undergoes a martensitic transformation $DO_3 \rightarrow 2H$ upon fast post recalescence cooling or a massive transformation $DO_3 \rightarrow DO_{19}$ upon slow cooling.

*L. Bendersky is with the Center for Materials Research, The Johns Hopkins University, Baltimore, Md. 21218 and the National Bureau of Standards, Gaithersburg, Md. 20899, as guest worker; T. Z. Kattamis is Professor, Institute of Materials Science, University of Connecticut, Storrs, Ct. 06268; and F. S. Biancaniello is with the National Bureau of Standards, Gaithersburg, Md. 20899.

To be published in Metallurgical Transations.

I. INTRODUCTION

The solidification microstructure of Co-34wt%Sn (Co-20.5at%Sn) eutectic alloy bulk-undercooled up to 250K prior to nucleation of the solid and cooled at 1 to 7 K/s after recalescence was previously studied.[1] It was found to consist of regions of anomalous eutectic surrounded by regions of lamellar eutectic. The amount of anomalous eutectic increased with undercooling and, to a lesser extent, with cooling rate. Both eutectics became finer with increasing undercooling and cooling rate. It was determined by electron microprobe analysis that both eutectics consisted of the same two phases: The cobalt-rich α-phase and the γ-Co_3Sn_2 phase. In the anomalous eutectic regions the α-phase appears in the form of particles dispersed within the γ-matrix. In specimens which were solidified at cooling rates exceeding approximately 3K/s the α-particles were interconnected, forming a relatively continuous network. At lower cooling rates the network became discontinuous because of extensive coarsening. The thermal stability of the network was further examined by isothermally holding a solidified specimen at 1348 K, approximately 37 K below the eutectic temperature, for about 10 h prior to water quenching. The α-phase network broke up into particles which quickly spheroidized. Microstructures of specimens which were undercooled 200K and cooled at 3 K/s after recalescence are illustrated in Figure 1. Figure 1b illustrates the microstructure of the specimen that

was originally solidified at an undercooling of 200K and was subsequently heat-treated at 1348K for 10h.

Remelting during recalescence,[2] as well as diffusion within the solid during and after recalescence which may lead to secondary phase precipitation modify the original microstructure of the freezing phase. It is only by minimizing these processes through rapid heat extraction that the original microstructure can be preserved and studied. In the investigation reported herein the alloy was melt-spun. For cobalt-base alloys which are known to undercool very readily, it is expected that the melt would undercool in contact with the wheel prior to nucleation of the solid. Undercooling would be combined with rapid heat extraction.

II. EXPERIMENTAL PROCEDURE

The alloy was melt-spun at 7200 rpm on a copper wheel (12×10^{-2}m dia). The ribbon was sectioned longitudinally and transversely, and studied metallographically. Analytical electron microscopy was used to characterize the structure and composition of phases present. Due to the brittleness of the material TEM specimens were prepared by ion milling. Because of the microstructural variations across the ribbon thickness two types of TEM specimens were prepared: (1) By milling from the chill side of the ribbon (bottom side) its top region was thinned down in order to study the microstructure corresponding to slower cooling conditions; (2) by milling from the top

side of the ribbon its bottom region was thinned down in order to study the microstructure corresponding to faster cooling conditions.

III. RESULTS

A longitudinal section of the ribbon is shown in Figure 2. The microstructure basically consists of columnar grains, 0.5-1 μm wide, which grow perpendicular to the ribbon surface in contact with the wheel. At some locations the columnar grains occupy the entire ribbon thickness, at some others, as in Figure 2, there is an abrupt interruption of the columnar grain structure and the upper region of the ribbon consists of a fine, optically unresolved granular structure. No intergranular phase was optically resolved. The darker appearance of grain boundaries was attributed to heavy etching.

Results of the electron microscopic examination may be summarized as follows:

(1) Microstructure of the Chill-Side of the Ribbon

Columnar grains grow perpendicular to the ribbon surface. A TEM micrograph illustrating a section of these grains parallel to the ribbon bottom surface is shown in Figure 3. No microsegregation was detected within or between these grains which underwent a martensitic transformation during solid state cooling. Such a transformation was not previously reported. X-ray energy dispersive analysis in STEM mode of the microscope indicated that the martensitic phase is of uniform composition,

expectedly equal to the nominal composition of the eutectic. A TEM specimen of this martensitic microstructure was, therefore, used as a composition standard for estimating the chemical composition of other unknown phases by EDAX-STEM. Diffraction analysis of the martensite indicated a 2H orthorhombic structure. This structure exhibited stacking faults on $(001)_{2H}$ plane and twins with $(121)_{2H}$ as twinning plane, Figures 3, 4 and 5.

(2) Microstructure of the Top Side of the Ribbon

At various locations of the ribbon the columnar grain structure is interrupted and the top side of the ribbon consists of a fine, optically unresolved microstructure, Figure 2. EDAX analysis of thin film of this side of the ribbon showed regions with a composition low in Sn and regions with a composition close to 41wt%Sn. It was decided that two phases were present. Additional electron microdiffraction analysis confirmed the presence of α-Co F.C.C. phase and of DO_{19} hexagonal phase which is isomorphous with low temperature Ni_3Sn. A TEM micrograph, Figure 6a, exhibits fine α-cobalt phase particles, less than 0.1 μm in size, dispersed in a matrix of composition close to 41wt%. This composition is very close to the stoichiometric composition of Co_3Sn.

(3) Microstructure of a Bulk-Undercooled and Heat-Treated Specimen

The microstructure of a bulk specimen (∿90 gm) which was solidified from a melt undercooled by about 200K, and was sub-

sequently heat-treated at 1348 K for 10 h and water-quenched, Figure 1b, consists of coarse, spheroidized particles of α-cobalt dispersed in a phase which was analyzed and found to contain 41wt%Sn. Analysis of electron diffraction patterns taken from the intermetallic phase (see Figure 7) yielded a DO_{19} structure, isomorphous with that of low temperature Ni_3Sn (Fig. 8a, b).

IV. DISCUSSION

The equilibrium phase diagrams of Sn with transition metals, Ni, Fe and Co are quite similar[3] and comprise a number of isotypical intermediate compounds. In Fe-Sn and Ni-Sn systems Fe_3Sn and Ni_3Sn are known phases. Because of this similarity, it is expected that Co_3Sn would also exist and assume the same structures as these two other intermetallic compounds.[5,6] A high temperature DO_3 structure, which undergoes a martensitic transformation to an orthorhombic 2H structure at high quench rates and a massive transformation to a low temperature DO_{19} hexagonal structure at lower cooling rates.

The cobalt-rich corner of the Co-Sn phase diagram is shown in Figure 9. It includes a new intermetallic phase with stoichiometric composition Co_3Sn which was recently reported in splat-cooled specimens[4] as having a BCC structure at room temperature. Unknown or inaccurately known phase boundaries and the two T_o curves are schematically represented in interrupted lines. It can be seen that at the eutectic composition

$T_{o_{Co_3Sn/L}}$ is higher than $T_{o_{\alpha\text{-}Co/L}}$. Thus, at this composition the undercooling required for partitionless solidification of Co_3Sn is less than that required for partitionless solidification of α-Co. It is, therefore, expected that Co_3Sn rather than α-Co would solidify from the undercooled melt, although interface attachment kinetics for cubic DO_3 are most likely slower than for the FCC α-Co phase. Co_3Sn would have a composition of 34wt%Sn instead of the stoichiometric 41wt%Sn, corresponding to a supersaturation in Co of about 7wt%. During recalescence solidification of Co_3Sn is partitionless up to a temperature T_o' lower than T_o, at which growth velocity falls below that required for solute trapping, D_L/a_o, where D_L is diffusion coefficient of Sn in the liquid and a_o is the interatomic dimension. Between T_o' and the maximum recalescence temperature, which for low undercoolings is almost as high as the eutectic temperature T_E = 1385 K, there is separation of the two phases: α-Co, which has a lower volume fraction and is particulate, and Co_3Sn (41wt%Sn) which forms the matrix. By analogy with Ni_3Sn[5,6] supersaturated Co_3Sn which forms below T_o' is expected to have a cubic DO_3 structure and to undergo a martensitic transformation during fast post-recalescence cooling. At high initial bulk undercooling and cooling rate the maximum recalescence temperature may not exceed T_o' and columnar grains of Co_3Sn (34wt%Sn), transformed into 2H martensite, would

occupy the entire ribbon thickness. At lower initial undercooling and cooling rate the maximum recalescence temperature may exceed T_o' in the top side of the ribbon and partitioning and phase separation would then take place, with α-Co regions dispersed in Co_3Sn (41wt%Sn) matrix. By analogy with Ni_3Sn this matrix would presumably be of DO_3 cubic structure and would undergo a massive transformation to DO_{19} hexagonal structure during solid state cooling. The maximum solubility limit in the α-Co phase may be extended. In splat-cooled Co-Sn alloys, the solid solubility in the α-Co phase reached 5at%Sn, exceeding the equilibrium solid solubility of 2.5at%Sn.[7]

A similar sequence of events would be expected for bulk-undercooled, slowly solidified ingots. Thus, because of lower undercooling or lower growth rate during recalescence partitioning would take place yielding a two-phase structure which consists of α-Co particles dispersed in a DO_{19}(41wt%Sn) matrix. In the bulk-undercooled and heat-treated specimen (1348K for 10h) the α-particles coarsened substantially.

V. SUMMARY

The microstructure of melt-spun ribbon of Co-34wt%Sn eutectic alloy consists of columnar grains of a supersaturated Co_3Sn martensitic 2H phase. These grains occupy the whole thickness of the ribbon, or the chill-side part of it, while the top part consists of a dispersion of supersaturated α-Co

particles in a DO_{19}(41wt%Sn) Co_3Sn hexagonal structure. This dispersion is similar to that observed in alloys solidified from bulk-undercooled melts and subsequently heat-treated. By analogy with Ni-Sn, a system which has several intermetallic compounds that are isomorphous with those of Co-Sn, a high temperature cubic DO_3 phase of Co_3Sn presumably forms and undergoes a martensitic transformation $DO_3 \rightarrow 2H$ upon fast cooling or a massive transformation $DO_3 \rightarrow DO_{19}$ upon slow cooling.

REFERENCES

1. Y. R. Murty and T. Z. Kattamis, J. Cryst. Growth, Vol. 22, 1974, p. 219.

2. T. Z. Kattamis, J. Cryst. Growth, Vol. 34, 1976, p. 215.

3. J.-F. Geny, G. Marchal, P. Mangin, Chr. Janot and M. Piecuch, Phys. Review B, Vol. 25, 1982, p. 7449.

4. G. Schluckebier, E. Wachtlel and B. Predel, Z. Mettallkde, Vol. 71, 1980, p. 456.

5. H. R. Pak, T. Saburi and S. Nenno, J. Jap. Inst. Metals, Vol. 37, 1973, p. 1128.

6. Y. Murakami and S. Kachi, Trans. Jap. Inst. Metals, Vol. 24, 1983, p. 9.

7. H.-L. Luo and P. Duwez, Can. J. Phys. Vol., 41, 1963, p. 758.

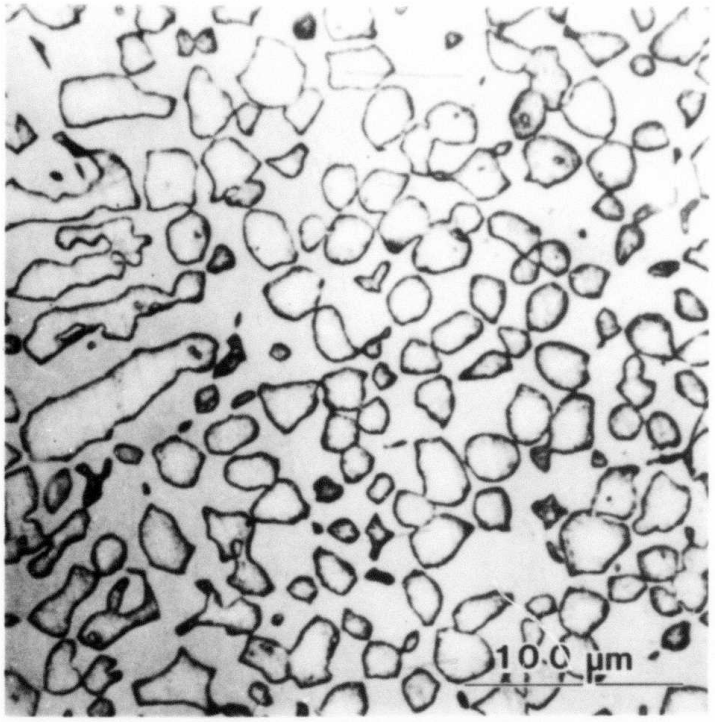

(a)

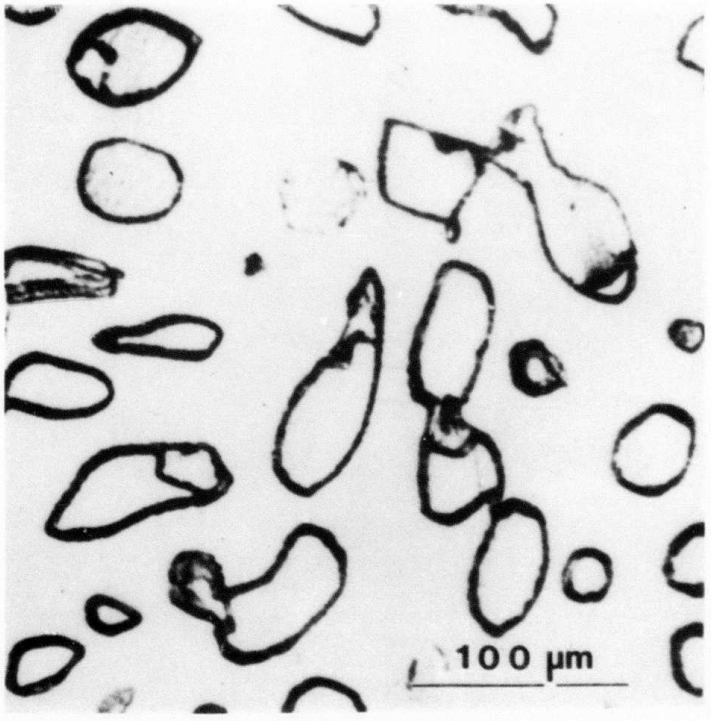

(b)

Figure 1: Photomicrographs of Co-34wt%Sn eutectic alloy specimens bulk-undercooled 200 K prior to nucleation of the solid. Cooling rates after recalescence were: 3K/s. Same specimen as in (a), following heat-treatment at 1348 K for 10 h and water-quenching (b).

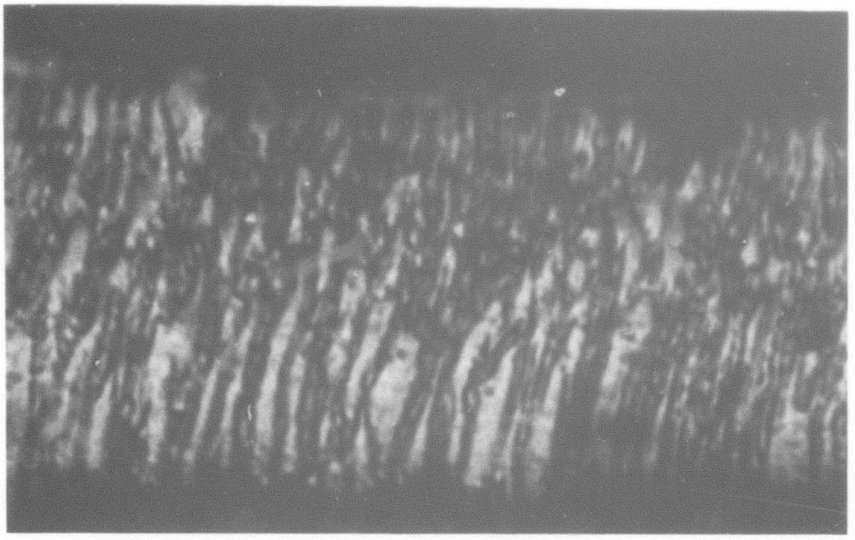

Figure 2: Photomicrograph of a longitudinal section of Co-34wt%Sn eutectic alloy melt-spun ribbon.

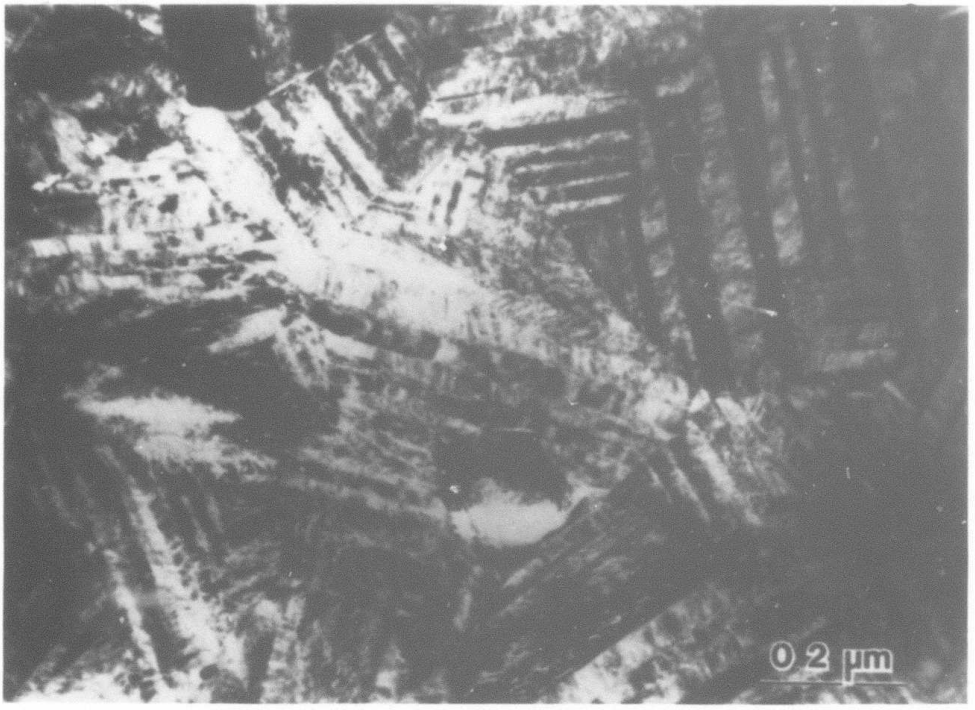

Figure 3: TEM micrograph of the chill-side of the ribbon illustrating columnar grains growing normal to the ribbon surface without microsegregation. These grains underwent a martensitic transformation during solid state cooling. Melt-spun Co-34wt%Sn eutectic alloy.

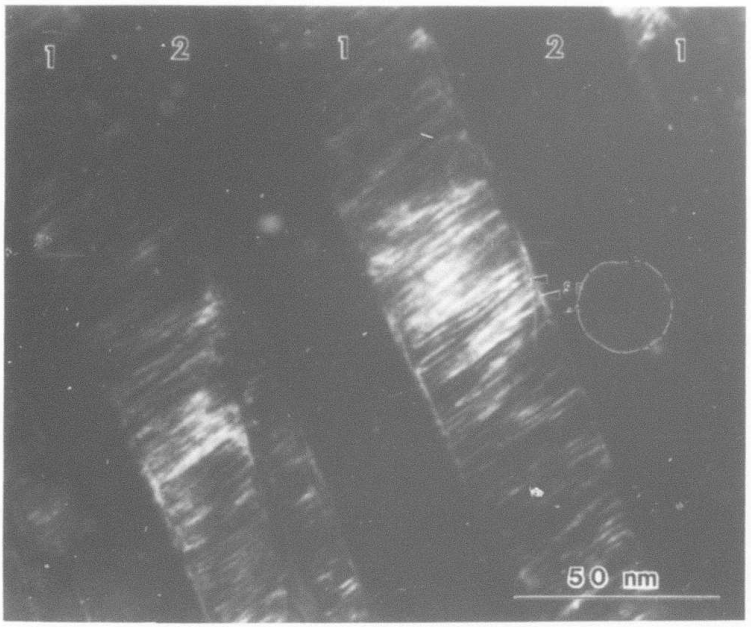

Figure 4: Dark field image of the 2H martensite. Twin variant 1 shows high density stacking faults.

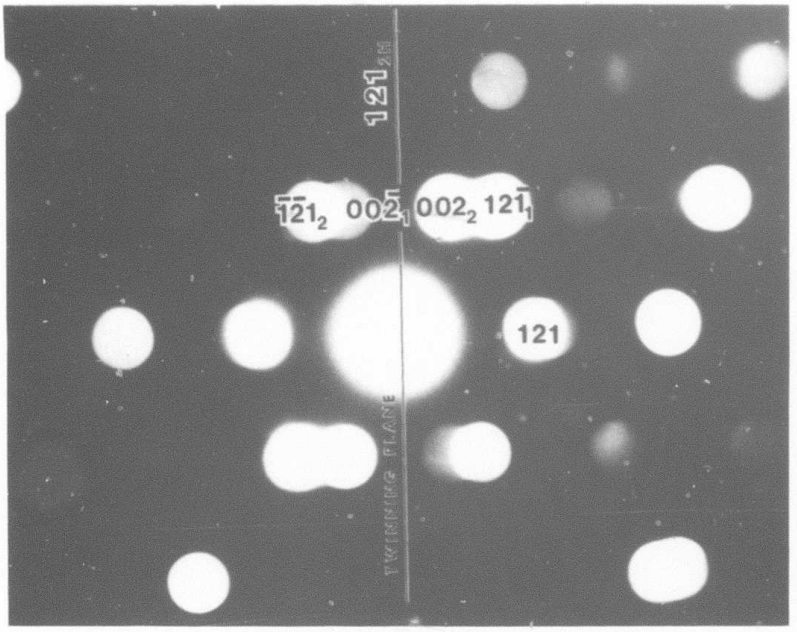

Figure 5: Microdiffraction pattern showing the existence of twins with $(121)_{2H}$ twinning plane.

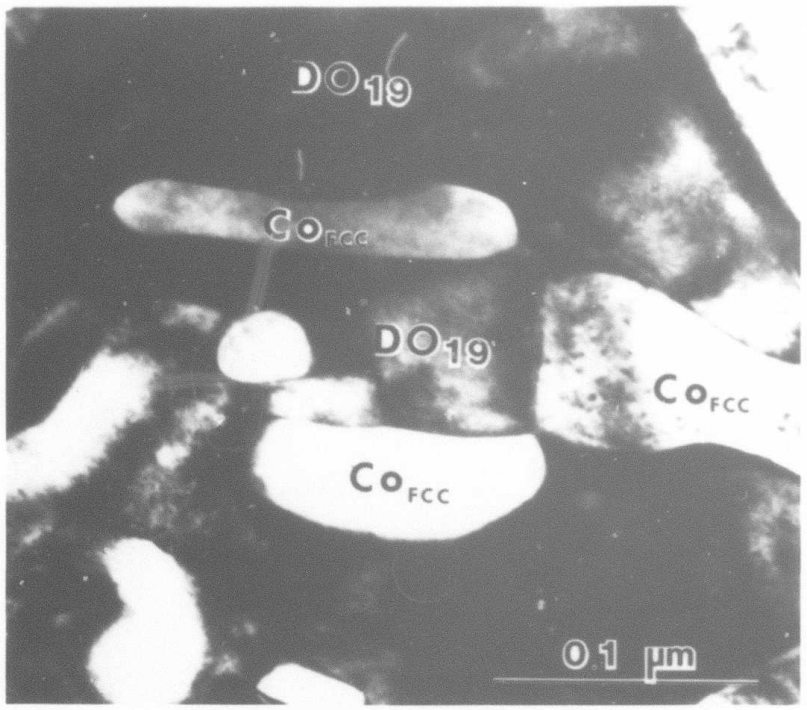

(a)

(b)

Figure 6: TEM micrographs of the top region of the ribbon. Melt-spun Co-34wt%Sn eutectic alloy.

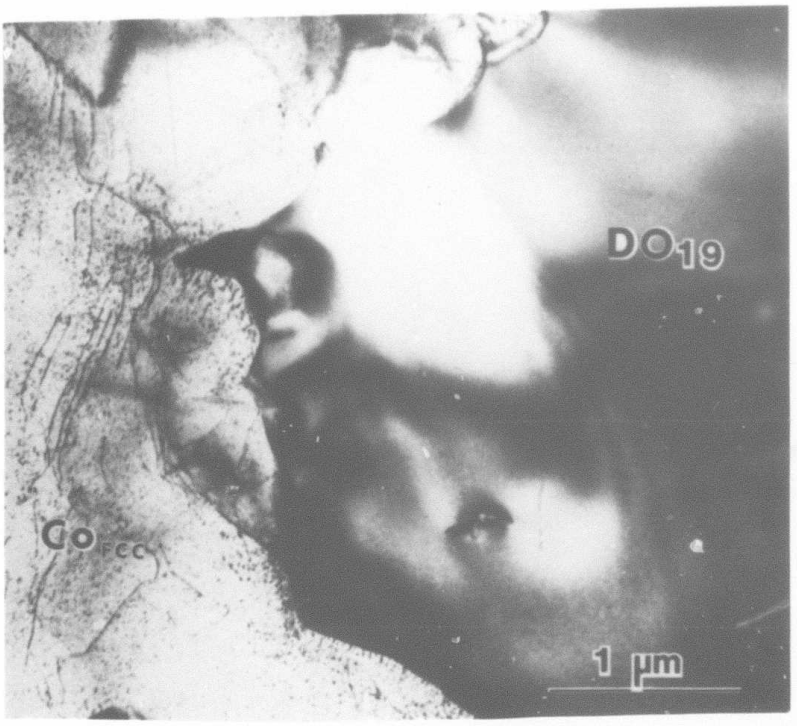

Figure 7: TEM micrograph of a specimen undercooled 200K and subsequently heat-treated at 1348K for 10h prior to water-quenching. Co-34wt%Sn eutectic alloy.

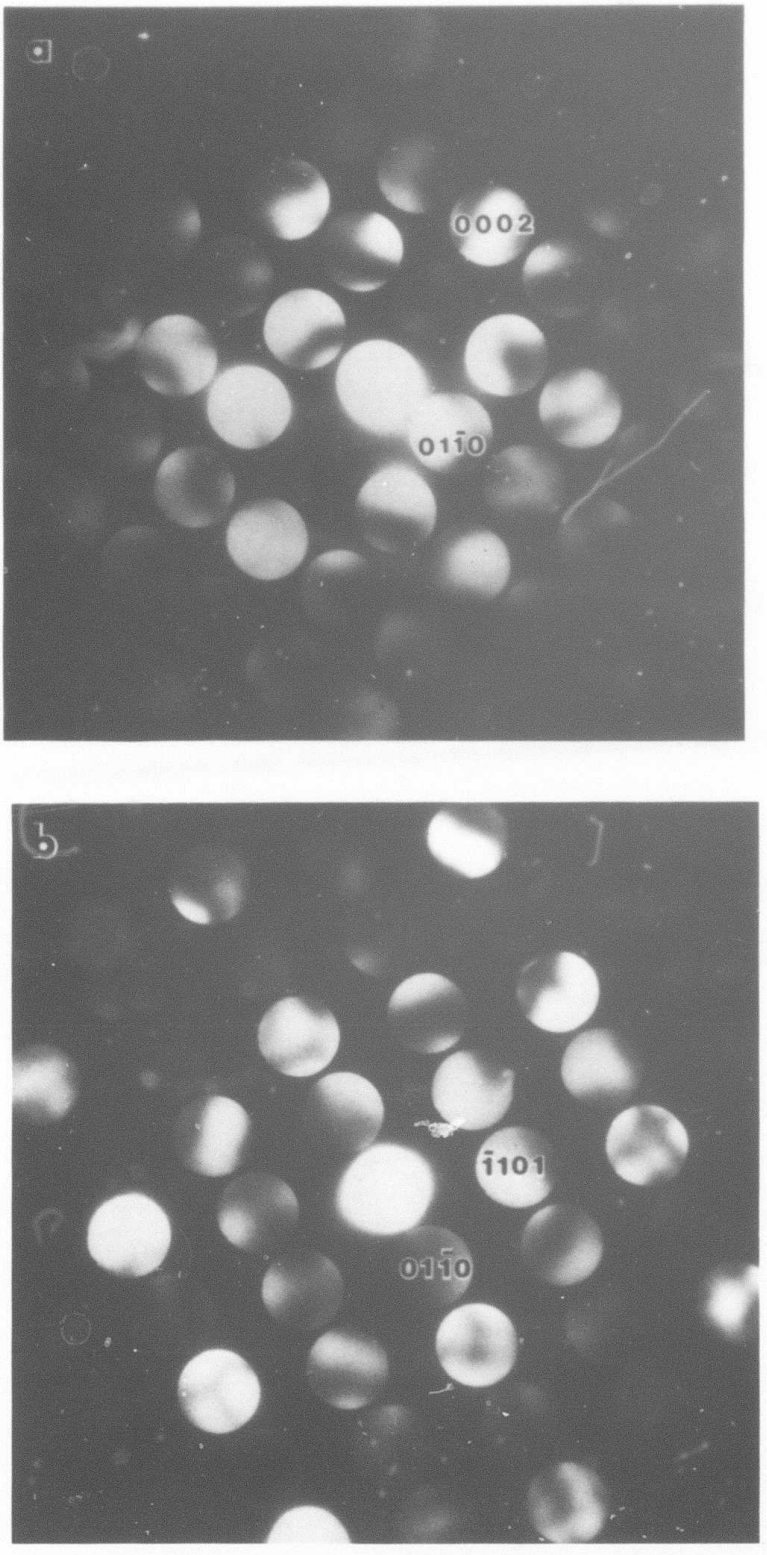

Figure 8: Electron diffraction patterns taken from intermetallic phase yielding hexagonal DO_{19} structure: (a) zone axis $2\bar{1}\bar{1}0$, (b) zone axis $2\bar{1}\bar{1}3$.

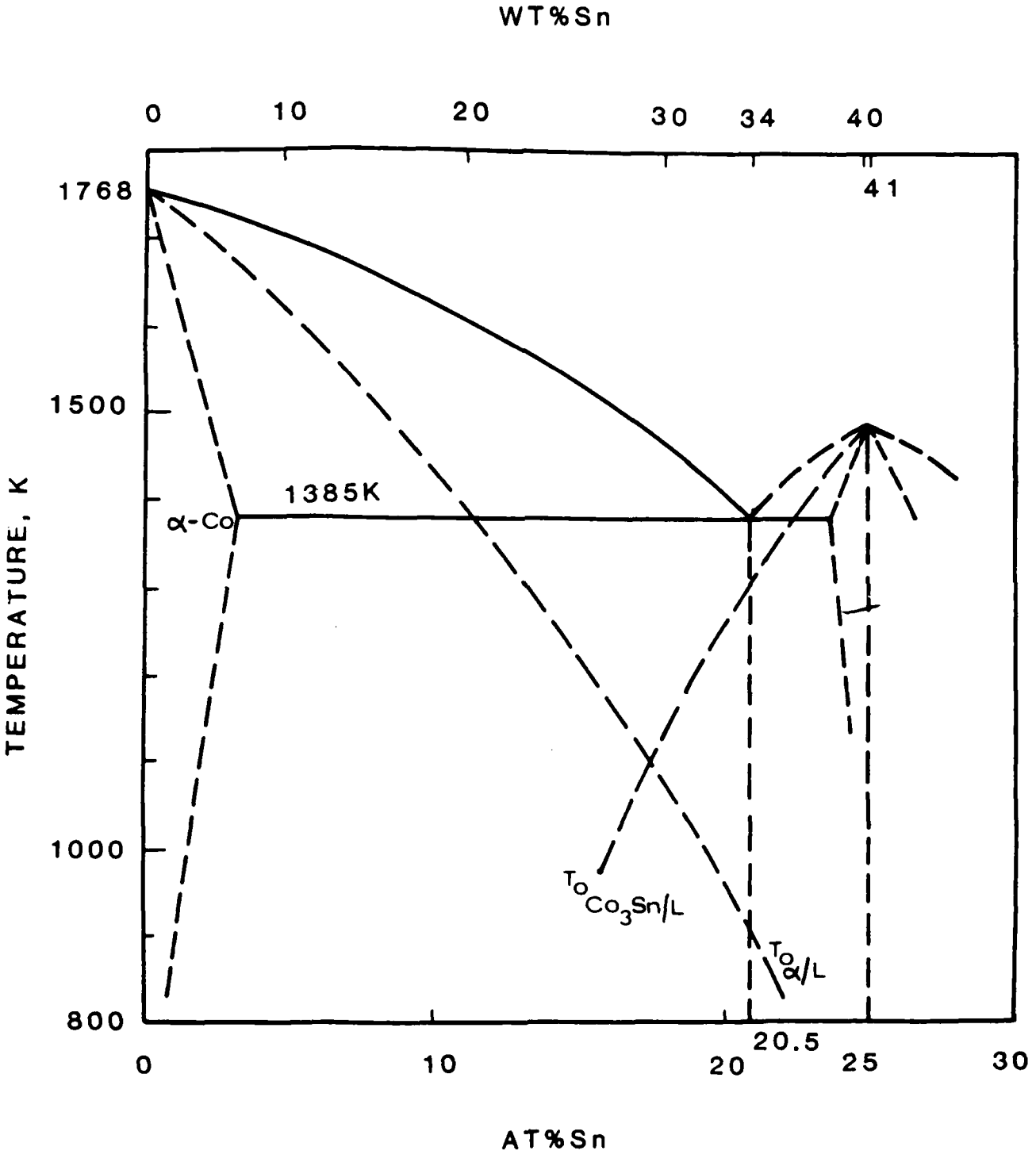

Figure 9 : The cobalt-rich corner of the Co-Sn phase diagram. Unknown phase boundaries are schematically represented in interrupted lines.

ALLOY PHASE DIAGRAMS, Proceedings of the MRS Meeting, Boston 1982, edited by L. H. Bennett, T. B. Massalski and B. C. Giessen, Elsevier (1983). P 265

METASTABLE PHASES IN RAPIDLY SOLIDIFIED ALUMINUM-RICH Al-Fe ALLOYS

O. SHECHTMAN* AND L.J. SWARTZENDRUBER+
*Johns Hopkins University, Baltimore, Maryland
+National Bureau of Standards, Gaithersburg, Maryland

ABSTRACT

Aluminum-rich Al-Fe binary alloys up to and including Al_3Fe were prepared by melt spinning in order to study the metastable phase structure and its transformation following heat treatment. Transmission electron microscopy and nuclear gamma-ray resonance were utilized in the study. The rapidly solidified structure was found to contain up to three metastable phases. One of the phases, with a composition and a gamma-ray resonance spectrum appropriate for Al_6Fe, has either a globular or a cellular morphology upon quenching.

INTRODUCTION

Because of the current and potential technological importance of metastable phases in aluminum alloys, rapid solidification of aluminum-rich alloys is being extensively studied. We report here some preliminary results from an examination of the Al-rich side of the Al-Fe phase diagram studied using transmission electron microscopy (TEM) and nuclear gamma-ray resonance (NGR). In the region up to about 41 w/o (25 a/o) Fe, current phase diagrams[1] indicate the existence of two stable phases, primary α-Al (with a minute amount of iron in solid solution) and Al_3Fe. Rapid solidification of Al-Fe alloys within the composition range of these two phases produces a number of metastable phases. Which particular phases form depends on the composition and on the solidification rate[2]. Compositions for this study were selected to extend previous results to higher iron concentrations at higher solidification rates.

EXPERIMENTAL

The alloys were rapidly solidified by chill block casting on a spinning copper wheel. The ribbons obtained were approximately 2 mm wide and 0.035 to 0.050 mm thick. Thin foils for transmission electron microscopy were prepared using a jet electropolishing unit and standard electrolyte at -40°C. All the ribbons were studied in a scanning transmission electron microscope (STEM). The information obtained included general images of the phase structure, selected area microdiffractions, and x-ray microanalysis of the composition of the main phases. Samples for nuclear gamma-ray resonance were prepared by cutting the ribbons into 6 mm lengths and placing them side by side to form a square approximately 6 mm on a side. The resulting samples had an areal density of ^{57}Fe between 0.05 and 0.1 mg/cm^2.

RESULTS

At 25 w/o Fe (Al_6Fe) and below, only two phases were found in the melt-spun alloys: α-Al solid solution with less than 1 w/o Fe, and an "S" phase with a composition near that of Al_6Fe. The diffraction pattern of the observed "S" phase does not appear to match the diffraction patterns for any of the previously reported aluminum-rich phases (Al_3Fe, Al_xFe, Al_6Fe, Al_9Fe_2, or Al_mFe) which form at lower solidification rates[2-3].

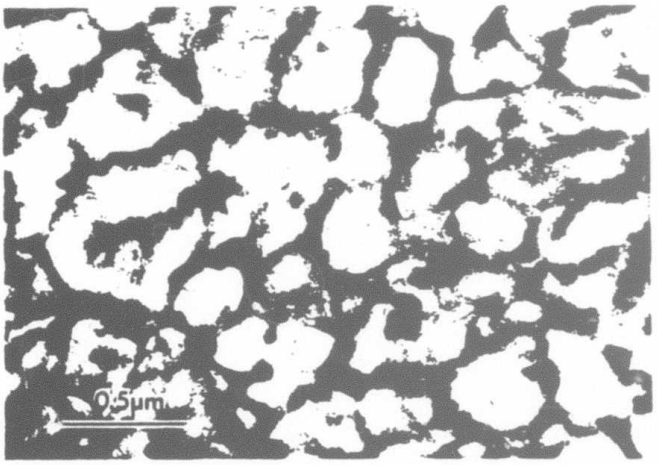

Fig. 1. Micrographs of melt-spun Al-9 w/o Fe showing the cellular structure which forms for alloys with up to 9 w/o Fe. The cells are α-Aluminum with a small amount of iron in solid solution, the cell walls are "S" phase.

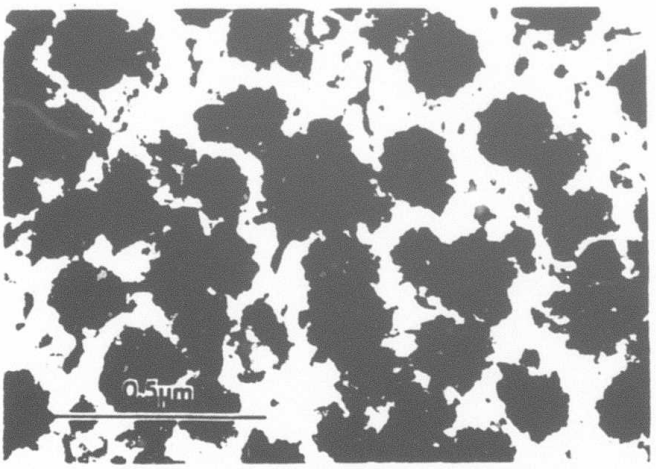

Fig. 2. Micrograph of melt-spun Al-12 w/o Fe showing the globular structure which forms for alloys with 12 or greater w/o Fe. In addition to the globules, a small amount of cellular structure similar to that of Figure 1 can be seen between the globules.

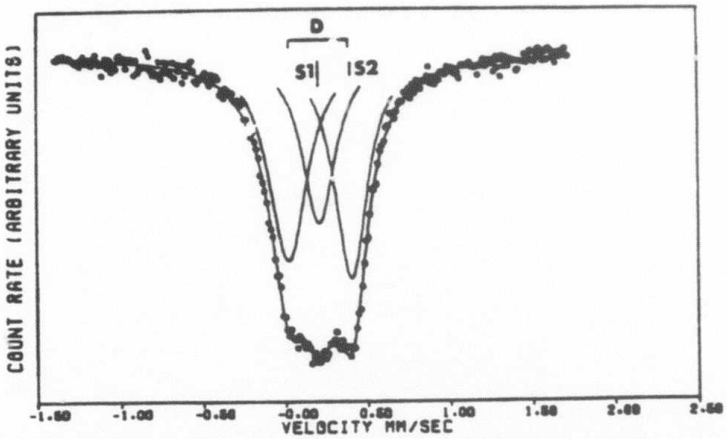

Fig. 3. NGR spectrum from a melt-spun alloy containing mostly Al_3Fe. The spectrum has been analyzed as a symmetric doublet , D, a singlet S1, and a singlet S2. The marking shown indicates the positions of the lines (but not their relative intensities).

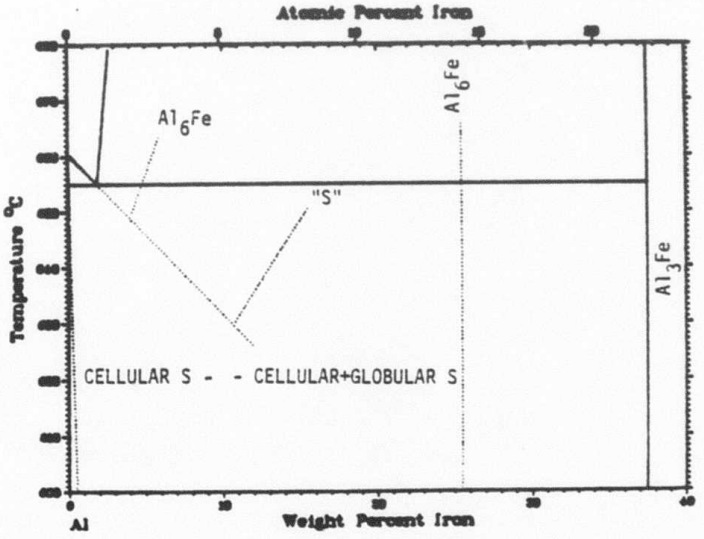

Fig. 4. A hypothetical metastable phase diagram for Al-rich aluminum iron alloys showing the approximate location of the metastable "S" phase eutectic between α-Al solid solution and the Al_6Fe composition of the "S" phase.

Below 9 w/o, a cellular structure (see Figure 1) is observed. The cells consist of α-Al solid solution and the cell boundaries of the "S" phase. At a composition between 9 and 12 w/o Fe a change in morphology of the melt-spun structure occurs. Above 12 w/o, a coarse primary globular phase of α-Al appears (see Figure 2), imbedded in the cellular structure. The globular phase appears to have a crystal structure and a composition identical to the "S" phase at the cell boundaries. At compositions above 25 w/o Fe, Al_3Fe is formed along with the globular "S" phase.

Throughout the range of compositions studied, the NGR spectra consist of three resolved lines. The spectra obtained here, along with previous results[4], indicate that the NGR pattern can be represented as the sum of Lorentzian shaped spectral lines arising from three separate contributions: (1) a nearly symetric doublet, D, plus a small amount of a singlet S1 (see Figure 3), both from the "S" phase; (2) the same nearly symmetric doublet, D, plus a large amount of the singlet S1, both from Al_3Fe; and (3) a singlet S2 from iron in solid solution in α-aluminum. Both the position and relative intensities of the doublet, D, and the singlet S1 are nearly identical for both the "S" phase and Al_6Fe. Thus the "S" phase probably can not be distinguished from Al_6Fe by the NGR spectra, however the relative amount of the S1 peak can be used to monitor the transition of the "S" phase to Al_3Fe as the material is heat treated and the appearance of the various contributions confirms the TEM results. The position of the doublet D and the singlet S1 from the "S" phase, from Al_6Fe, and from Al_3Fe are nearly identical, indicating a very similar local structural and electronic environment for the iron atoms in these phases. The iron atoms are of two basic types, one with a non-cubic local environment yielding a quadrupole doublet, and the other a more symmetric environment yielding a singlet.

A hypothetical metastable phase diagram is shown in Figure 4. The liquidus and solidus have been extended by dotted lines. It is known that the formation of Al_3Fe can be suppressed even at low cooling rates and Al_6Fe forms with the approximate eutectic temperature and compostion shown. At the high solidification rates achieved in the melt-spun alloys, the formation of Al_6Fe is suppressed and the "S" phase forms. The appearance of the primary globules of "S" phase in the microstructure above 12 w/o Fe suggests a possible metastable eutectic between liquid, α-Al, and "S" at ~10.5 w/o Fe. Due to kinetic factors, such as an assymetric coupled zone (common for Al-Fe alloys), this composition should be considered an upper bound. Between the metastable eutectic and 25 w/o Fe, the cellular and globular "S" are observed. Above 25 w/o Fe only globular "S" and Al_3Fe are observed in the melt-spun alloys. Further studies are underway to quantify the phases present, to determine the effect of heat treatment, and to extend the results with ternary additions.

ACKNOWLEDGEMENTS

We wish to thank F.S. Biancanello for alloy preperation and W.J. Boettinger, J.L. Murray, and L.H. Bennett for valuable discusssions. We acknowledge the support of DARPA for this study.

REFERENCES

1. M. Hansen and K. Anderko, "Constitution of Binary Alloys", McGraw Hill, New York, 1958, p. 91.
2. R.M.K. Young and T.W. Clyne, Scripta Met. 15, 1211 (1981).
3. T.R. Anantharaman, P. Ramachandrarao, C. Suryanarayana, S. Lele, and K. Chattapadhyay, Trans. Indian Inst. of Metals 30, 423 (1977).
4. C. Janot and H. Gilbert, Phil. Mag. 27, 545 (1973).

AMS/AIME MEETING, TORONTO, CANADA, OCTOBER 1985

ABSTRACT

THE MICROSTRUCTURE OF RAPIDLY SOLIDIFIED Aℓ-3.7 wt% Ni-1.5 wt% Fe

L. Bendersky*, W. J. Boettinger**, R. J. Schaefer**,
and F. S. Biancaniello**

Microstructural variations in Aℓ-3.7 wt% Ni-1.5 wt% Fe alloys obtained by electron beam solidification passes at speeds between 5 m/s and 1 mm/s are determined. These variations are very similar to those observed across melt spun ribbons and in atomized powders. Four general microstructural types are observed with increasing solidification velocity: primary intermetallic $Aℓ_9(Fe,Ni)_2$, eutectic of α-Aℓ and $Aℓ_9(Fe,Ni)_2$, cellular α-Aℓ and α-Aℓ supersaturated with Fe and Ni. The latter microstructure is frequently observed to contain fine dispersions of $Aℓ_9(Fe,Ni)_2$ presumably formed during solid-state decomposition of the supersaturated α-Aℓ phase. The effect of solidification velocity on the microstructure will be analyzed.

*Center for Materials Research, The Johns Hopkins University, Baltimore, Md. 21218.

**Metallurgy Division, National Bureau of Standards, Gaithersburg, Md. 20899.

This research is supported by DARPA.

AMS/AIME MEETING, TORONTO, CANADA, OCTOBER 1985

ABSTRACT

POSSIBLE STRUCTURAL SIMILARITIES BETWEEN THE VARIOUS PHASES PRODUCED IN Aℓ-Mn ALLOYS USING A RANGE OF SOLIDIFICATION CONDITIONS

L. Bendersky*, M. J. Kaufman** and R. J. Schaefer**

The recent discovery by Shechtman, et al. [1] of a phase having apparent icosahedral ($m\bar{3}\bar{5}$), non-crystallographic symmetry in rapidly solidified Aℓ-Mn alloys has sparked a great amount of interest and controversy concerning the detailed structure and properties of this phase. In the present work, similar alloys were solidified using a range of cooling rates and examined in order to study the structures of the other non-equilibrium phases and determine whether any similarities exist between them and that of the icosahedral phase. The results indicate that at least two other intermediate metastable phases are produced at slower rates of cooling (these have been termed T and T'). These two phases along with both the icosahedral and the stable $Aℓ_4Mn$ (hexagonal, a = 2.7 nm, c = 1.2 nm, point and space groups unknown) phases have been examined using a variety of experimental techniques including conventional, analytical and high resolution transmission electron microscopy. The results indicate that many structural similarities indeed do exist between the various phases and these will be described in some detail.

*Center for Materials Research, Johns Hopkins University, Baltimore, Md. 21218.

**National Bureau of Standards, Gaithersburg, Md. 20899

This research is supported by DARPA.